

Library Unit  
9. 073287 R.O.1

47

44

CONFIDENTIAL

Copy  
RM SL54K29

NACA RM SL54K29

R.A. A 13247 R.O.1

UNCLASSIFIED

MDC CONTROL  
NO. C-227026



# RESEARCH MEMORANDUM

FOR REFERENCE

for the

NOT TO BE TAKEN FROM THIS ROOM

U. S. Air Force

EFFECTS OF WING LEADING-EDGE CAMBER AND TIP MODIFICATIONS  
ON THE AERODYNAMIC CHARACTERISTICS OF A 1/20-SCALE  
MODEL OF THE CONVAIR F-102 AIRPLANE AT TRANSONIC SPEEDS

By Kenneth E. Tempelmeyer and Robert S. Osborne

Langley Aeronautical Laboratory  
Langley Field, Va.

CLASSIFIED DOCUMENT

This material contains information affecting the National Defense of the United States within the meaning of the espionage laws, Title 18, U.S.C., Secs. 793 and 794, the transmission or revelation of which in any manner to an unauthorized person is prohibited by law.

NATIONAL ADVISORY COMMITTEE  
FOR AERONAUTICS  
WASHINGTON

CONFIDENTIAL

UNCLASSIFIED



3 1176 01438 6792

## NATIONAL ADVISORY COMMITTEE FOR AERONAUTICS

## RESEARCH MEMORANDUM

for the

U. S. Air Force

## EFFECTS OF WING LEADING-EDGE CAMBER AND TIP MODIFICATIONS

## ON THE AERODYNAMIC CHARACTERISTICS OF A 1/20-SCALE

## MODEL OF THE CONVAIR F-102 AIRPLANE AT TRANSONIC SPEEDS

By Kenneth E. Tempelmeyer and Robert S. Osborne

## SUMMARY

The effects of several wing leading-edge camber and deflected-tip modifications on the force and moment characteristics of a 1/20-scale model of the Convair F-102 airplane have been determined at Mach numbers from 0.60 to 1.14 for angles of attack up to  $14^\circ$  in the Langley 8-foot transonic tunnel. The effects of elevator deflections from  $0^\circ$  to  $-10^\circ$  were also obtained for a configuration incorporating favorable leading-edge and tip modifications.

Leading-edge modifications which had a small amount of constant-chord camber obtained by vertically adjusting the thickness distribution over the forward (3.9 percent of the mean aerodynamic chord) portion of the wing were ineffective in reducing the drag at lifting conditions at transonic speeds. Leading edges with relatively large cambers designed to support nearly elliptical span load distributions at lift coefficients of 0.15 and 0.22 near a Mach number of 1.0 produced substantial reductions in drag at most lift coefficients. Their effectiveness was indicated by a 16- to 25-percent increase in the maximum lift-drag ratio as compared with the basic configuration. A small portion of the drag reduction and a 5-percent increase of the maximum lift-drag ratio were due to the extension of the leading edge required for installation of these types of camber. Deflecting the wing-tip trailing edge outboard of 82 percent of the semispan upward approximately  $10^\circ$  about the elevator hinge line extended had a favorable effect on the trim drag. Large reductions in drag due to lift and drag due to trim were indicated for a modified wing configuration with leading edges cambered to support a nearly elliptical span load distribution at a lift coefficient of 0.15 near a Mach number of 1.0 in conjunction with tips deflected upward  $10^\circ$ . Leading-edge and tip modification, in general, had little effect on the lift characteristics of the basic configuration. Chordwise fences which essentially eliminated pitch-up tendencies on a plane delta wing were not adequate on some of the cambered wings.

UNCLASSIFIED

## INTRODUCTION

At the request of the U. S. Air Force, an investigation has been made in the Langley 8-foot transonic tunnel to determine the stability, control, and performance characteristics of a 1/20-scale model of the Convair F-102 airplane. The results of the initial tests (refs. 1 and 2) indicated the original configuration had high transonic drag at zero lift, high drag due to lift, and high drag due to trim. It was apparent that, in order to improve the medium- and high-altitude performance of the configuration, all three should be appreciably reduced. Body modifications based upon the area-rule concept and designed to reduce the transonic zero-lift drag of the original configuration have been tested, and the results are reported in reference 3.

The present tests were conducted to determine the aerodynamic effects of several cambered wing leading edges designed to reduce the drag due to lift and of several wing-tip modifications designed to reduce the drag due to trim. Reported herein are the force and moment characteristics of the configurations tested for Mach numbers from 0.60 to 1.14 and angles of attack up to  $14^\circ$ . Also presented are the results of limited elevator-deflection tests for a modified configuration employing both leading-edge and tip modifications.

## SYMBOLS

|           |  |
|-----------|--|
| A         | aspect ratio   |
| $A_E$     | duct exit area, sq ft  |
| b         | wing span, in.   |
| $C_{D_m}$ | measured drag coefficient adjusted to free-stream static pressure at model base, $D_m/q_S$ |
| $C_{D_I}$ | internal drag coefficient, $D_I/q_S$   |
| $C_D$     | external drag coefficient, $C_{D_m} - C_{D_I}$   |
| $C_{D_0}$ | external drag coefficient at zero lift   |
| $C_{D_T}$ | trimmed external drag coefficient  |

|                                  |   |
|----------------------------------|---|
| $C_{D_{\delta=0}}$               | external drag coefficient with $0^\circ$ elevator setting   |
| $\Delta C_D$                     | trim drag reduction   |
| $C_L$                            | lift coefficient, $L/qS$  |
| $C_{L(L/D)_{\max}}$              | lift coefficient for maximum lift-drag ratio  |
| $\partial C_L / \partial \alpha$ | lift-curve slope per degree averaged from $C_L = 0$ over linear portion of the curve                                |
| $C_m$                            | pitching-moment coefficient, $M_{cg}/qS\bar{c}$   |
| $\partial C_m / \partial C_L$    | static longitudinal stability parameter   |
| $\partial C_m / \partial \delta$ | elevator-effectiveness parameter at constant lift coefficient   |
| $\bar{c}$                        | wing mean aerodynamic chord, in.  |
| $D_m$                            | measured drag adjusted to free-stream static pressure at the model base, lb   |
| $D_I$                            | internal drag, $m(V_O - V_E) - A_E(p_E - p_O)$ , lb   |
| $K$                              | drag-due-to-lift factor, $\partial C_D / \partial C_L^2$  |
| $L$                              | lift, lb  |
| $(L/D)_{\max}$                   | maximum lift-drag ratio   |
| $M$                              | free-stream Mach number   |
| $M_{cg}$                         | pitching moment about center-of-gravity location at $0.275\bar{c}$ and $0.036\bar{c}$ above wing-chord plane, in-lb |
| $m$                              | mass flow through inlets, slugs/sec   |
| $m_o$                            | mass flow in free-stream tube of area equal to projected inlet area at $\alpha = 0^\circ$ , slugs/sec               |
| $m/m_o$                          | inlet mass-flow ratio   |

|          |  |
|----------|--|
| $p_E$    | static pressure at duct exit, lb/sq ft   |
| $p_O$    | free-stream static pressure, lb/sq ft  |
| $q$      | free-stream dynamic pressure, lb/sq ft   |
| $S$      | wing area including area in fuselage, sq ft (See table I.)   |
| $V_E$    | velocity in duct exit, ft/sec  |
| $V_O$    | free-stream velocity, ft/sec   |
| $\alpha$ | angle of attack of basic wing-chord line, deg  |
| $i_t$    | wing-tip setting, negative when trailing edge is up, deg   |
| $\delta$ | elevator deflection, measured at right angles to hinge line and negative when trailing edge is up, deg |

#### APPARATUS AND METHODS

##### Tunnel and Model Support System

The tests were conducted in the Langley 8-foot transonic tunnel which is a single-return wind tunnel with a dodecagonal slotted throat permitting continuous operation through the speed of sound. The tunnel operates at approximately atmospheric stagnation pressures. Details of test section design and flow uniformity can be found in reference 4.

The model was attached (through an internal strain-gage balance) to a sting support which was cylindrical for 3.2 base diameters downstream of the model base. The sting support was fixed axially in the center of the tunnel by two sets of struts projecting from the tunnel walls. By employing angled couplings in the sting, the model position was maintained close to the tunnel axis at all angles of attack.

##### Model

Basic configuration.- The 1/20-scale model used in this investigation was supplied by the contractor. Geometric characteristics of the basic configuration are presented in figure 1 and table II. The axial variation of cross-sectional area of the model is available in reference 3.

The basic model had a delta wing with  $60^\circ$  sweptback leading edges,  $5^\circ$  sweptforward trailing edges, and NACA 0004-65 (modified) streamwise airfoil sections (see ref. 1). The wing was constructed with a tin-bismuth surface formed over a steel core and had duralumin leading edges and steel tips that were removable. Chordwise fences (described in ref. 1) were located at the 66-percent wing semispan station. (See fig. 1.) The vertical tail had the same plan form and airfoil sections as the wing semispan. Longitudinal control was provided by wing trailing-edge flaps deflected about a hinge line perpendicular to the model center line. The total flap area rearward of the hinge line was 10.2 percent of the total wing area, and the gap ahead of the hinge line was sealed.

The fuselage was equipped with twin ram-jet inlets and internal ducting which allowed air flow from the model base. In order to insure that the air flow would not be critical at the jet exit with the sting in place, the fuselage boattail angle was decreased and the base diameter increased 0.3 inch as compared with an exact 1/20-scale model. Also it should be noted that, as a result of modifications to the full-scale airplane after the model had been constructed, the model tested contained several compromises with respect to an exact 1/20-scale model. (See ref. 3.)

Wing leading-edge modifications.— Dimensional details of the wing plan forms incorporating the various leading edges are given in figure 2 and table I. Streamwise airfoil sections of the leading-edge modifications and the basic leading edge are compared at three wing semispan stations in figure 2. The rear camber lines noted in figure 2 separate the cambered from the uncambered portions of the wing. The type of chordwise fence employed with these various modifications is listed in table I.

Leading-edge modifications 1, 2, and 3 were developed from low-speed tests by the contractor, required no change in the basic-wing plan form, and made use of the removable anti-icing leading-edge section. Modification 1 had a constant-chord camber from the wing-fuselage juncture to the 82-percent wing-semispan station which was obtained by sliding the thickness distribution of the removable leading edge (the forward 0.535 in. of the model streamwise airfoil section and 0.0398) vertically until its lower surface was parallel to the basic chord line. The basic leading-edge radius was retained.

Modification 2 had one-half the leading-edge droop at 15.21 percent of the semispan and the same droop at 60 percent of the semispan as modification 1 had; a linear distribution of droop through these two points continued to 82 percent of the semispan. The thickness distribution was adjusted vertically to give a straight-line lower surface over the cambered (forward 0.535 in.) portion of the wing.

Modification 3 had the same camber as modification 2 and had the lower surface built up to increase the leading-edge radius on the order of 50 percent.

Leading-edge modifications 4, 5, and 6 were designed by using the theoretical considerations presented in reference 5 based on linearized lifting-surface theory. These modifications required extending the leading edge of the basic-wing plan form with no change in primary wing structure.

Modification 4 had conical camber extending from the root to the tip with a parabolic spanwise mean line over the outboard 10 percent of the local semispan. The amount of leading-edge droop was equal to the theoretical value required to support a nearly elliptical spanwise load distribution at a lift coefficient of 0.22 near a Mach number of 1.0. The thickness distribution was obtained by linearly stretching the wing nose section from the rear camber line to the new leading edge.

Modification 5 had a constant chord-extension with the same amount of leading-edge droop as required by theory for a design lift coefficient of 0.15 near a Mach number of 1.0. The leading-edge camber extended from the root to the tip and was obtained from a parabolic chordwise mean line, the apex of the parabola being 0.535 inch rearward of the basic leading edge. The thickness distribution was obtained by linearly stretching the forward 0.535 inch of the basic streamwise airfoil section to the new leading edge.

Modification 5a had the same plan form and thickness distribution as modifications 5 and 6 but was uncambered. It was tested to isolate the effects of plan-form change from the effects of camber.

Modification 6 had the same plan form and thickness distribution as modification 5. It had conical camber extending from the root to the tip, a parabolic distribution of the camber over the outboard 6.37-percent local semispan, and had the amount of leading-edge droop required for a design lift coefficient of 0.15 at a Mach number near 1.0.

Wing-tip modifications.— The wing-tip modifications (see fig. 3 and table I) extended from the 82- to the 100-percent semispan stations and were selected on the basis of low-speed model tests by the contractor. These tip modifications were tested with the basic leading edges applied from the root to the 82-percent-semispan station.

Modification A had the same leading-edge camber as modification 2 but the camber was applied from the 82-percent-semispan station to the tip. The trailing edge of the tip was deflected up at angles of  $0^\circ$ ,  $5^\circ$ ,  $9^\circ$ , and  $15^\circ$  about the elevator hinge line extended. The portion of the wing deflected comprised 1.5 percent of the total basic-wing area.

Modification B had plain basic leading edges. The entire tip, which was 3 percent of the total basic-wing area, was rotated about the 50-percent local-chord station at 82 percent of the semispan to  $7.5^\circ$  negative incidence with respect to the basic chord line.

Additional details concerning the leading-edge and tip modifications are available in reference 6.

Modified wing configuration.- The modified wing had the same leading-edge camber as modification 6 and the trailing edge of the tip was deflected up  $10^\circ$  about the elevator hinge line extended. The chordwise fences were extended to the wing leading edge.

### Measurements and Accuracy

Normal force, axial force, and pitching moment were measured with an internal strain-gage balance. The pitching moment was measured about a center-of-gravity location at 27.5 percent of the mean aerodynamic chord and 3.6 percent of the mean aerodynamic chord above the wing-chord plane on the basic model. These data were reduced to lift, drag, and pitching-moment coefficients based on the actual wing area and mean aerodynamic chord of the individual configuration (see table I) and the above center-of-gravity location. The force and moment coefficients for all configurations are estimated to be accurate within the following limits up to a lift coefficient of at least 0.4:

|           |       |             |
|-----------|-------|-------------|
| $C_L$     | ..... | $\pm 0.005$ |
| $C_{D_m}$ | ..... | $\pm 0.001$ |
| $C_m$     | ..... | $\pm 0.001$ |

Mass flow through the ducts and internal drag were determined from total-pressure and static-pressure measurements obtained with a survey rake located at the model base. The accuracy of the internal drag coefficients was estimated to be within 0.001.

The angle of attack was determined to within  $0.15^\circ$  from a pendulum inclinometer located in the support sting and a calibration of sting and balance deflection with respect to model load. The elevator control deflections are estimated to be accurate within  $0.2^\circ$ .

The Mach number was determined to within 0.003 from a calibration with respect to test chamber pressure.

### Tests

All configurations were tested with the ducts open. The Mach numbers ranged from 0.60 to 1.14. The angle of attack for the basic configuration varied from  $0^\circ$  to about  $10^\circ$  and for the configurations with the various leading-edge and tip modifications from the angle of zero lift to approximately  $11^\circ$ . Internal-flow characteristics were measured for the basic configuration only at angles of attack from  $0^\circ$  to  $9^\circ$ .

The modified wing configuration was tested with elevator deflections of  $0^\circ$ ,  $-5^\circ$ , and  $-10^\circ$  at angles of attack from the angle of zero lift up to  $14^\circ$ .

A range of test Reynolds numbers based on the mean aerodynamic chords of the various wing plan forms (see table I) is shown in figure 4. The average Reynolds number was of the order of  $4.4 \times 10^6$ .

### Corrections

The slotted test section minimizes boundary interference at subsonic speeds, and no corrections for this interference have been applied.

The effects of supersonic boundary-reflected disturbances were reduced by testing the model a few inches off the tunnel center line. These disturbances were too weak to have any appreciable effect at a Mach number of 1.025 and had moved downstream from the model at a Mach number of 1.14. However, the reflected disturbances probably caused small errors in the drag and pitching-moment measurements at a Mach number of 1.075. These errors have been minimized by fairing the data plotted against Mach number and it is believed that the trends shown by these faired data are free of boundary-reflected disturbances.

No sting-interference corrections have been applied to these data. The sting effects should be small, however, because the flow from the internal ducting system surrounds the sting when it is discharged at the model base.

As previously noted, the model tested was not an exact scale model replica of the prototype airplane. (See ref. 3.) This model deviation would affect the magnitude of the transonic drag but should have little effect on the other aerodynamic characteristics. An estimate of the error in drag due to the model deviation was obtained by the method presented in reference 7 and is shown for the basic configuration in figure 5. The validity of this correction has been substantiated by comparison with flight test data for the Convair F-102 airplane (ref. 8). Although this is an estimate of the error in minimum drag (near zero lift), it is probably valid for low lifting conditions also. This correction has not been applied to the data herein.

### RESULTS AND DISCUSSION

The lift coefficients required for level flight have been calculated for the Convair F-102 airplane with a combat wing loading of 35.4 pounds per square foot at altitudes from sea level to 60,000 feet and are presented in figure 6.

The results of this investigation are presented in the following figures:

|   | Figure   |
|---|----------|
| Internal flow characteristics:                            |          |
| Mass-flow ratios and internal drag coefficients . . . . . | 7        |
| Force and moment characteristics:                         |          |
| Effects of leading-edge modifications . . . . .           | 8 to 10  |
| Effects of tip modifications . . . . .                    | 11       |
| Effects of elevator deflection . . . . .                  | 12       |
| Summary and analysis figures: .                           |          |
| Effects of leading-edge modifications . . . . .           | 13 to 15 |
| Effects of tip modifications . . . . .                    | 16       |
| Effects of elevator deflection . . . . .                  | 17 to 21 |

The drag data for all configurations used in the summary and analysis plots (figs. 13 to 19) have had the internal drag of the configuration with basic (plain) leading edges and tips and zero elevator deflection removed (fig. 7). It was assumed that the wing modifications and elevator deflections would have no effect on the internal-flow characteristics of the model.

In order to present the data compactly, sliding scales have been used in many of the figures and care should be taken in selecting the zero axis of each curve. Only a portion of the data has been faired in order to keep the figures easily readable.

#### Effects of Leading-Edge Modifications

The drag due to lift of plane delta wings is generally considerably higher than would be expected from theoretical considerations because of flow separation over the leading edge and the attendant loss of leading-edge suction or thrust. As indicated in reference 9, it is possible to reduce the drag due to lift of  $60^\circ$  delta wings for Mach numbers up to 1.4 by employing cambered leading edges designed to produce elliptical spanwise load distributions. The beneficial effect of camber is associated with a reduction in leading-edge separation and therefore an increase in lift and suction forces over the leading edge. In addition, leading-edge camber usually produces an increase in the pitching moment at zero lift which results in a decrease in out-of-trim pitching moment and a reduction in trim drag.

Because of similarity of type of camber, the leading-edge modifications presented herein are compared with the basic leading-edge configuration in two groups. The effects of plan form are isolated from the effects of camber in a third grouping.

Modifications 1, 2, and 3.- The analysis plots of figure 13 present the trends indicated for modifications 1, 2, and 3 by a cross-hatched band.

Modifications 1, 2, and 3 generally reduced the drag coefficients of the model at lift coefficients above about 0.1 but increased the drag at lower lift coefficients (fig. 8(a)). The magnitude of the drag reduction was relatively small, especially at Mach numbers above 0.9 (see fig. 13(a)). All these camber modifications increased the maximum lift-drag ratios about 5 percent over the speed range (fig. 13(b)) but had little effect on the lift coefficients at which the maximum lift-drag ratios occurred. It is evident that these modifications were relatively ineffective in reducing the drag at lifting conditions for the Convair F-102 model in the transonic range. The amount of camber for this type of leading edge was considerably less than that of reference 8 and, apparently, was not large enough to alter the flow phenomena over the leading edge at transonic speeds appreciably.

The effects of modifications 1, 2, and 3 on the lift characteristics of the model were small and consisted primarily of a 4-percent decrease in the average lift-curve slope (fig. 13(c)).

The pitching-moment curves at high subsonic Mach numbers indicated an increase in stability for configurations with modifications 1, 2, and 3 at lift coefficients above about 0.3 (fig. 8(c)). It should be observed that these cambers did not produce the previously mentioned beneficial decrease in out-of-trim pitching moment.

Modifications 4, 5, and 6.- The lift-drag polars of figures 9(a) indicated that modifications 4, 5, and 6 produced substantial reductions in drag coefficient at most lifting conditions tested. The expected increase in zero-lift drag due to cambering the leading edges was larger at subcritical than at transonic speeds (fig. 14(a)). Notably, modifications 5 and 6 actually decreased the zero-lift drag at Mach numbers above 1.025. This decrease was probably the result of the plan-form change inherent in these modifications which decreased the airfoil-section thickness ratio and wing aspect ratio and, as will be shown in a subsequent section, decreased the transonic drag rise. At a lift coefficient of 0.2 the modifications reduced the drag coefficient about 0.004 over the speed range. At a lift coefficient of 0.4 the reductions were much larger; modification 6, for example, decreased the drag coefficient of the model about 0.016 at a Mach number of 0.90 and 0.010 at a Mach number of 1.075. These data also indicated that the effectiveness of the modifications decreased with increasing Mach number.

When the individual modifications of the extended leading-edge group (figs. 9(a) and 14(a)) are compared, it is of interest to note that modifications 5 and 6 were designed for the same lift coefficient and Mach

number (hence, the same physical leading-edge droop) and exhibited nearly identical drag characteristics although the parabolic camber line was streamwise in the former case and spanwise in the latter. Modification 4 was designed for a higher lift coefficient, and the data indicated that, with respect to modifications 5 and 6, the lift-drag polar was rotated slightly clockwise so that the drag was higher at low lift coefficients and lower in the higher lift range. It is significant that the favorable effects of these leading-edge modifications were obtained by cambering less than the outboard 20 percent of the local semispan indicated in reference 5. The leading-edge droop was effective with as little as the outboard 6.37 percent of the semispan cambered.

This group of modifications increased the maximum lift-drag ratios an average of 25 percent at a Mach number of 0.60 and 16 percent at a Mach number of 1.075 (fig. 14(b)). The lift coefficient for maximum lift-drag ratio was increased approximately 0.05 by the modifications.

It was evident that these camber modifications were responsible for sizable reductions in the drag at lifting conditions. Selecting the optimum cambered leading edge was difficult, however, since no single modification had an overall superiority. Modification 6 was preferred by the contractor because of a combination of aerodynamic and structural considerations.

All leading-edge modifications in this group increased the angle of attack for zero lift about  $0.4^\circ$  throughout the Mach number range (fig. 9(b)) but, except for modification 4, had little effect on the average lift-curve slope (fig. 14(c)). Modification 4, probably because of the more significant plan-form change, produced consistently higher lift-curve slopes over the speed range.

At high subsonic Mach numbers the pitching-moment curves (fig. 9(c)) indicate a range of neutral stability with possible pitch-up tendencies for modifications 4 and 6 at lift coefficients greater than 0.4. The chordwise fences for the basic (plain) leading-edge wing were unaltered for this part of the investigation and, therefore, did not begin at the leading edge of the wings with modification 4, 5, or 6. For the elevator-deflection tests, the chordwise fences were extended to the leading edge of the modified wing but there was no improvement in the neutral stability region. (See figures 12(a), 12(b), and 12(c).) Thus, the neutral stability for modifications 4 and 6 appears to be an effect of camber, and the chordwise fence used was not adequate. Effects of the modifications on the static longitudinal stability parameter were small and consisted primarily of slight decreases in stability for the modifications 5 and 6 (fig. 14(c)).

Modifications 5, 5(a), and 6. - The change in plan form (modification 5(a)) which decreased the airfoil-section thickness ratio and wing aspect ratio produced drag reductions throughout most of the test range

as compared with the basic configuration (fig. 10(a)). At Mach numbers above 1.0, the influence of the plan-form change was increased since at supersonic speeds the drag is proportional to the airfoil-section thickness ratio squared. The transonic drag rise decrease at low lift coefficients (see fig. 15(a)) indicated that the plan-form change reduced the low-lift drag penalty associated with camber. Camber alone was apparently responsible for most of the drag reduction at lift coefficients above 0.2. Modification 5(a) increased the maximum lift-drag ratio over the basic configuration only about 5 percent as compared with approximately 16 to 25 percent for modifications 5 and 6 (fig. 15(b)).

In order to indicate the effectiveness of the more successful cambers, the theoretical best possible maximum lift-drag ratio and the value for no leading-edge suction for the wing with the uncambered leading-edge extension (modification 5(a)) have been added to figure 15(b) for comparison. Theoretical values of the maximum lift-drag ratio were computed from

$$(L/D)_{\max} = \frac{1}{2\sqrt{KC_{D_0}}} \quad \text{where } K \text{ (drag-due-to-lift factor) for full leading-}$$

edge suction was taken as  $\frac{1}{\pi A}$  for subsonic speeds and obtained from reference 10 for supersonic speeds. For no leading-edge suction  $K$  was assumed equal to  $\frac{1}{57.3 \frac{\partial C_L}{\partial \alpha}}$ . At subcritical speeds, the maximum lift-drag

ratios for the cambered leading-edge configurations (especially modification 5) were very near the theoretical maximum. This result illustrates the effectiveness of this type of camber and indicates that large additional drag-due-to-lift reductions could not be expected by altering these modifications. At the higher speeds, the cambered wings produced about 50-percent full leading-edge suction or approximately three times as much as that for the plain leading-edge wing of the same plan form.

There were no significant changes in the lift characteristics of the basic model due to the change in plan form (figs. 10(b) and 15(c)).

The pitching-moment curves (fig. 10(c)) show a region of neutral stability for uncambered modification 5(a) similar to that for the cambered modification 6. It is believed that the decrease of stability for modification 5(a) was associated with the chordwise fences not extending to the leading edge; extending the fences would probably provide adequate stability. Extension of the wing leading edge moved the center of pressure forward and resulted in a .015c forward shift in the aerodynamic-center location for modifications 5, 5(a), and 6 (fig. 15(c)).

### Effects of Tip Modifications

Increased pitching moment may be obtained for a control surface of a given type and location by increasing the control-surface deflection or by increasing the control surface area, both of which have an approximately linear variation with pitching moment. Inasmuch as the drag varies as a linear function of control area and as the square with control deflection, it follows that increasing the control area in some manner should have a favorable effect on the drag penalty paid for a given pitch increment. For this reason fixed deflection tip modifications which, in effect, increased the control surface area were proposed as a means of reducing the trim drag of the F-102 configuration.

The faired data for modification A with  $i_t = 0^\circ$  were essentially the same as the basic configuration data. Therefore, in order to simplify the figures, modification A with  $i_t = 0^\circ$  has been used as the basis for tip comparisons.

The data of figures 11(a) and 11(c) indicate that the tips produced sizable positive increments of pitching moment with only small increases in drag. These drag increases were equal to or usually smaller than the drag penalty produced by equal pitch increments obtained by elevator deflections (see ref. 2); therefore, decreases in trim drag should be realized from these tip modifications. In order to indicate the effectiveness of each tip, it was assumed there was no interference between the tips and elevators and the trim drag reduction produced by the tip modifications was calculated for the configuration of reference 2. These calculations indicated that modification A with a deflection of approximately  $-10^\circ$  was optimum if emphasis is placed on the cruise and high-altitude performance of the F-102 airplane. Reductions in the trim drag coefficient as high as approximately 0.004 were indicated at a Mach number of 0.6 at an altitude of 40,000 feet (fig. 16).

There were no unusual effects of the tip modifications on the aerodynamic parameters of the basic configuration. (See figs. 11(a), 11(b), and 11(c).).

### Effects of Elevator Deflection

Limited elevator-deflection tests were made on a configuration incorporating the same wing leading edges as modification 6 and tip trailing edges deflected  $10^\circ$  upward about the elevator hinge line extended. These wing modifications were selected as optimum by the contractor from aerodynamic and structural considerations. This configuration is referred to hereinafter as the "modified wing configuration" and is compared with the

original model of reference 2 which had plain leading edges and tips. This comparison was made in order to indicate the overall reductions in drag which have been obtained with respect to the original model.

Drag.- As would be expected from previous discussion of the cambered leading edges and deflected tips, use of the modified wing with elevators undeflected resulted in small increases in minimum drag coefficient and appreciable decreases in drag at lifting conditions as compared with the basic plain wing configuration. (Compare figs. 12 and 9(a).)

Trimmed lift-drag polars for the modified wing configuration are compared with similar polars for the configuration of reference 2 in figure 17. Although it must be considered that the present model had an improved canopy and nose which reduced the transonic zero-lift drag rise approximately 0.002 as compared with the model of reference 2, it is readily apparent that the trimmed total drag for the present model has been significantly reduced at all Mach numbers tested; increases of approximately 32 percent in trimmed maximum lift-drag ratio are indicated in figure 18. Although the cambered leading edges and deflected tips have resulted in less drag due to trim for the present configuration as compared with the model of reference 2, it is indicated in figure 17 that the drag penalty for trimming the airplane is still sizable at lift coefficients above 0.2.

The effects of the wing modifications on the various components comprising the total trimmed drag for level flight of the F-102 airplane at an altitude of 40,000 feet for a wing loading of 35.4 pounds per square foot (corresponding to lift coefficients varying from 0.36 at  $M = 0.6$  to 0.1 at  $M = 1.14$ ) are indicated in figure 19. The minimum drag has been adversely affected by the modifications while the drag due to lift and drag due to trim have both been reduced, the largest reduction being in drag due to trim. These data indicate that, even with possible decreases in the effects of the modifications due to full-scale Reynolds numbers, appreciable increases in maximum speed, range, and altitude should be realized by application of the modifications to the airplane.

Lift.- The lift curves for the various elevator deflections were generally linear over the lift range covered in this investigation. The lift-curve slope increases from 0.046 at a Mach number of 0.60 to a peak of 0.056 at a Mach number of 1.0 for the model with the elevators undeflected. Trimming the configuration reduced the lift-curve slope as much as 10 percent to 30 percent (fig. 20). As stated in reference 2, this large reduction was due to the large loss of lift incurred when the elevators, which comprise about 10 percent of the wing area, are deflected upward to obtain trim. The trimmed lift-curve slopes for the modified wing configuration were approximately 10 percent higher than those for the configuration of reference 2.

Pitching moment.- As previously stated, the chordwise fences were extended to the leading edge of the wing for these elevator-deflection tests, but the region of neutral static longitudinal stability indicated for modification 6 was not changed (fig. 12). In the trim lift range, however, the pitching-moment curves were generally linear at all elevator deflections.

The value of static longitudinal stability parameter  $\partial C_m / \partial C_L$  for the modified wing configuration in level flight at 40,000 feet varied from -0.075 at a Mach number of 0.60 to about -0.180 at a Mach number of 1.14; thus, a rearward shift of the aerodynamic-center location of about 11 percent of the mean aerodynamic chord (fig. 21) was indicated. The wing modifications did not change the magnitude of this shift, but they did cause the shift to be much more gradual over the Mach number range as compared with the model with the plain wing.

The elevator pitch effectiveness parameter  $\partial C_m / \partial \delta$  was measured at constant lift coefficient and was averaged over the elevator-deflection range for lift coefficients from 0 to 0.4 (fig. 21). The elevator pitch effectiveness for the modified wing configuration reached a peak at a Mach number of about 0.90 but then decreased 35 percent as the Mach number increased to 1.0. The characteristics were similar to those indicated for the model of reference 2.

## CONCLUSIONS

Wind-tunnel tests conducted to determine the effects of several leading-edge camber and deflected tip modifications on the aerodynamic characteristics of a 1/20-scale model of the Convair F-102 airplane at transonic speeds indicated the following conclusions:

1. Small amounts of constant-chord leading-edge camber obtained by vertically sliding the thickness distribution until the lower surface was approximately flat over the forward (3.9 percent of the mean aerodynamic chord) portion of the wing were ineffective in reducing the drag due to lift at transonic speeds.
2. Leading-edge modifications with relatively large amounts of camber designed from linearized theory to support nearly elliptical span load distributions at lift coefficients of 0.15 and 0.22 near a Mach number of 1.0 produced sizable reductions in drag at lifting conditions. These modifications, which also required extension of the leading edge, were responsible for a 16- to 25-percent increase in the maximum lift-drag ratio over the speed range.

3. The change in wing plan form required for application of a linearized theory camber reduced the drag slightly over the lift range and was responsible for 5 percent of the 16- to 25-percent increase in the maximum lift-drag ratio.

4. Deflected tip modifications produced small reductions in the trim drag. Tip trailing edges deflected about the elevator hinge line extended to an angle of approximately  $-10^{\circ}$  appeared to be optimum.

5. Leading-edge camber designed from linearized theory for a lift coefficient of 0.15 near a Mach number of 1.0 in conjunction with tip trailing edges deflected upward  $10^{\circ}$  about the elevator hinge line extended produced large reductions in drag due to trim and drag due to lift. The maximum trimmed lift-drag ratios of the basic configuration were increased about 32 percent over the speed range by these modifications.

6. There were, in general, no significant changes in lift characteristics due to any of the leading-edge and tip modifications. The pitching-moment data indicated that, for adequate stability, wings cambered according to linearized theory would require a different type of fence than a plane delta wing.

Langley Aeronautical Laboratory,  
National Advisory Committee for Aeronautics,  
Langley Field, Va., November 10, 1954.

*Kenneth E. Tempelmeyer*

Kenneth E. Tempelmeyer  
Aeronautical Research Scientist

*Robert S. Osborne*

Robert S. Osborne  
Aeronautical Research Scientist

Approved:

*Eugene C. Draley*  
Eugene C. Draley

Chief of Full-Scale Research Division

sam

## REFERENCES

1. Osborne, Robert S., and Wornom, Dewey E.: Aerodynamic Characteristics Including Effects of Wing Fixes of a 1/20-Scale Model of the Convair F-102 Airplane at Transonic Speeds. NACA RM SL54C23, U. S. Air Force, 1954.
2. Osborne, Robert S., and Tempelmeyer, Kenneth E.: Longitudinal Control Characteristics of a 1/20-Scale Model of the Convair F-102 Airplane at Transonic Speeds. NACA RM SL54G15, U. S. Air Force, 1954.
3. Kelly, Thomas C., and Osborne, Robert S.: Effects of Fuselage Modifications on the Drag Characteristics of a 1/20-Scale Model of the Convair F-102 Airplane at Transonic Speeds. NACA RM SL54K18a, U. S. Air Force, 1954.
4. Ritchie, Virgil S., and Pearson, Albin O.: Calibration of the Slotted Test Section of the Langley 8-Foot Transonic Tunnel and Preliminary Experimental Investigation of Boundary-Reflected Disturbances. NACA RM L51K14, 1951.
5. Hall, Charles F., and Heitmeyer, John Charles: Lift, Drag, and Pitching Moment of Low-Aspect-Ratio Wings at Subsonic and Supersonic Speeds - Twisted and Cambered Triangular Wing of Aspect Ratio 2 With NACA 0003-63 Thickness Distribution. NACA RM A51E01, 1951.
6. Burnett, H. R.: Geometry of Cambered Leading Edges and Warped Tips To Be Evaluated in the NACA 8 Ft. and 4 x 4 Ft. Tunnels for the F-102 Airplane. Aero Memo A-8-44 (Contract AF33(600)-5942), Consolidated Vultee Aircraft Corp., May 27, 1953.
7. Nelson, Robert L., and Stoney, William E., Jr.: Pressure Drag of Bodies at Mach Numbers up to 2.0. NACA RM L53I22c, 1953.
8. Wesesky, John L. and Stephens, Robert L.: Phase II Flight Tests of the YF-102 Airplane S/N USAF No. 52-7995. AF Tech. Rep. No. AFFTC 54-14, Air Force Flight Test Center (Edwards, Calif.), July 1954.
9. Hall, Charles F.: Lift, Drag, and Pitching Moment of Low-Aspect-Ratio Wings at Subsonic and Supersonic Speeds. NACA RM A53A30, 1953.
10. Jones, Robert T.: Estimated Lift-Drag Ratios at Supersonic Speed. NACA TN 1350, 1947.

TABLE I.- GEOMETRIC CHARACTERISTICS OF VARIOUS WING MODIFICATIONS

| Configuration   | Type of Modification           | Wing area,<br>sq ft | $\bar{c}$ , in. | Aspect<br>ratio | Leading-edge<br>sweep | Fence             |
|-----------------|--------------------------------|---------------------|-----------------|-----------------|-----------------------|-------------------|
| Modification 1  | Leading-edge camber            | 1.625               | 13.755          | 2.2             | 60°                   | Basic             |
| Modification 2  | Leading-edge camber            | 1.625               | 13.755          | 2.2             | 60°                   | Basic             |
| Modification 3  | Leading-edge camber            | 1.625               | 13.755          | 2.2             | 60°                   | Basic             |
| Modification 4  | Leading-edge camber            | 1.713               | 13.622          | 2.1             | 57.69°                | Basic             |
| Modification 5  | Leading-edge camber            | 1.715               | 14.146          | 2.1             | 60°                   | Basic             |
| Modification 5a | Leading-edge extended          | 1.715               | 14.146          | 2.1             | 60°                   | Basic             |
| Modification 6  | Leading-edge camber            | 1.715               | 14.146          | 2.1             | 60°                   | Basic             |
| Modification A  | Tip                            | 1.625               | 13.755          | 2.2             | 60°                   | Basic             |
| Modification B  | Tip                            | 1.625               | 13.755          | 2.2             | 60°                   | Basic             |
| Modified Wing   | Leading-edge camber<br>and tip | 1.715               | 14.146          | 2.1             | 60°                   | Extended<br>basic |

TABLE II.- DIMENSIONS OF THE 1/20-SCALE MODEL OF THE  
CONVAIR F-102 AIRPLANE

Basic (plain) wing:

|   |                         |
|---|-------------------------|
| Airfoil section . . . . .   | NACA 0004-65 (modified) |
| Total area, sq ft . . . . .   | 1.625                   |
| Aspect ratio . . . . .  | 2.2                     |
| Taper ratio . . . . .   | 0                       |
| Incidence, deg . . . . .  | 0                       |
| Dihedral, deg . . . . .   | 0                       |
| Longitudinal location of center of<br>gravity, percent $\bar{c}$ . . . . .                      | 27.5                    |
| Vertical location of the center of<br>gravity above the wing chord, percent $\bar{c}$ . . . . . | 3.6                     |
| Elevator area back of the hinge line, sq ft . . . . .   | 0.166                   |

Vertical tail:

|                               |                         |
|-------------------------------|-------------------------|
| Airfoil section . . . . .     | NACA 0004-65 (modified) |
| Exposed area, sq ft . . . . . | 0.1704                  |
| Aspect ratio . . . . .        | 1.1                     |
| Taper ratio . . . . .         | 0                       |

Fuselage:

|  |        |
|--|--------|
| Frontal area (without canopy), sq ft . . . . .               | 0.075  |
| Fineness ratio . . . . .                                     | 8.2    |
| Projected inlet area at $\alpha = 0^\circ$ , sq ft . . . . . | 0.0111 |
| Duct exit area (excluding sting), sq ft . . . . .            | 0.0196 |

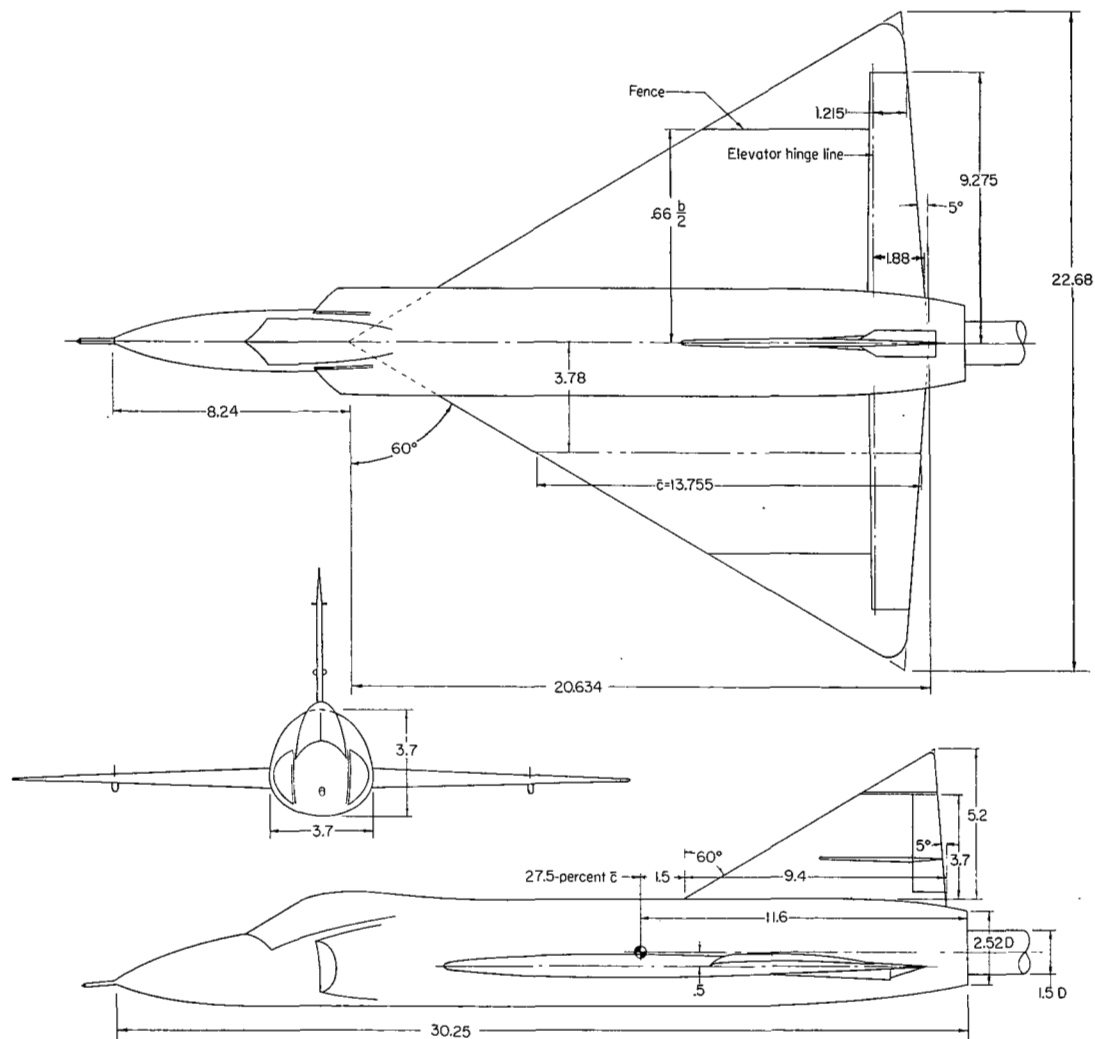
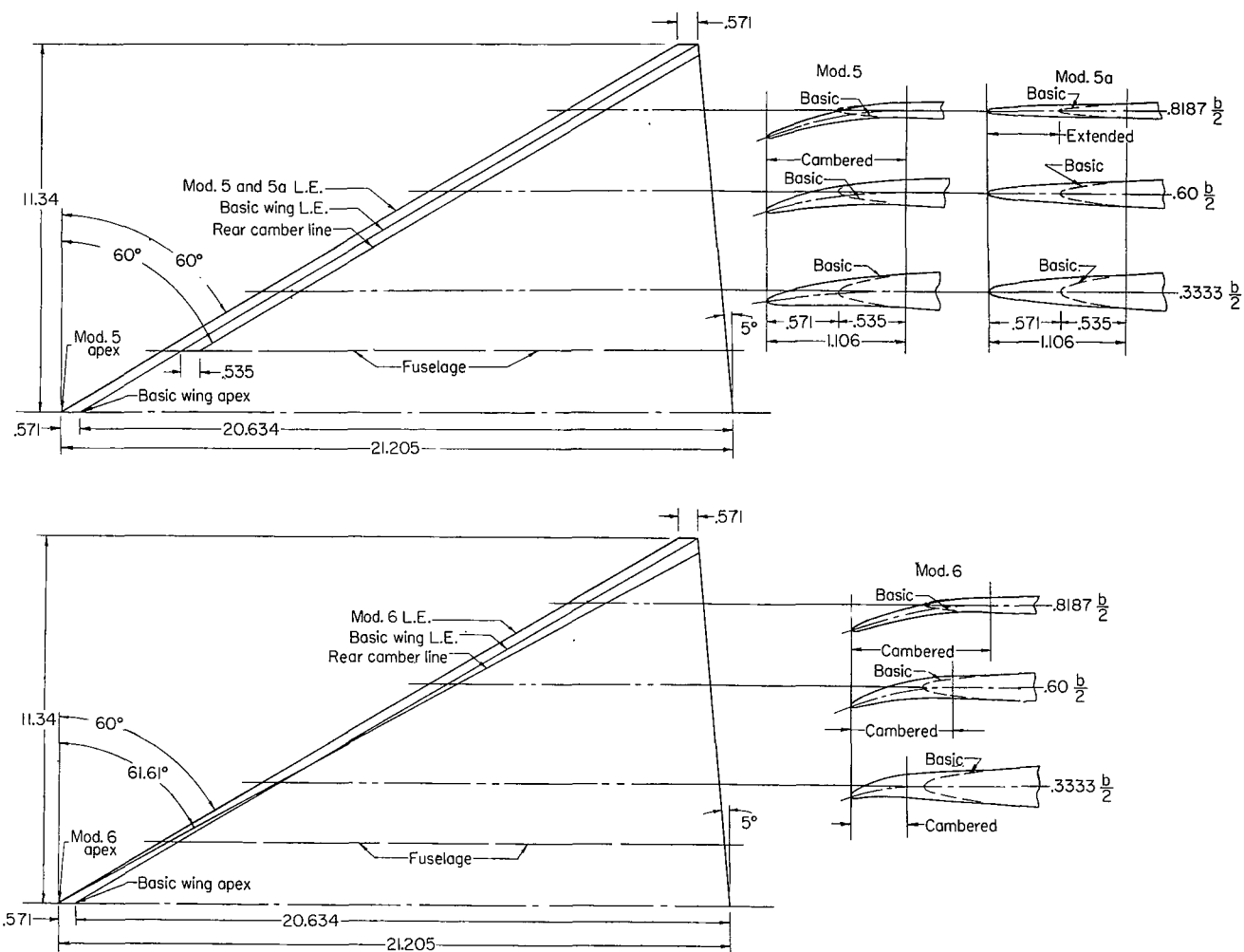


Figure 1.- Model details. All dimensions are in inches unless otherwise noted.



(a) Modifications 1, 2, 3, and 4.

Figure 2.- Dimensional details of leading-edge modifications. All dimensions are in inches unless otherwise noted. Plan form and streamwise airfoil sections are not to same scale.



(b) Modifications 5, 5a, and 6.

Figure 2.- Concluded.



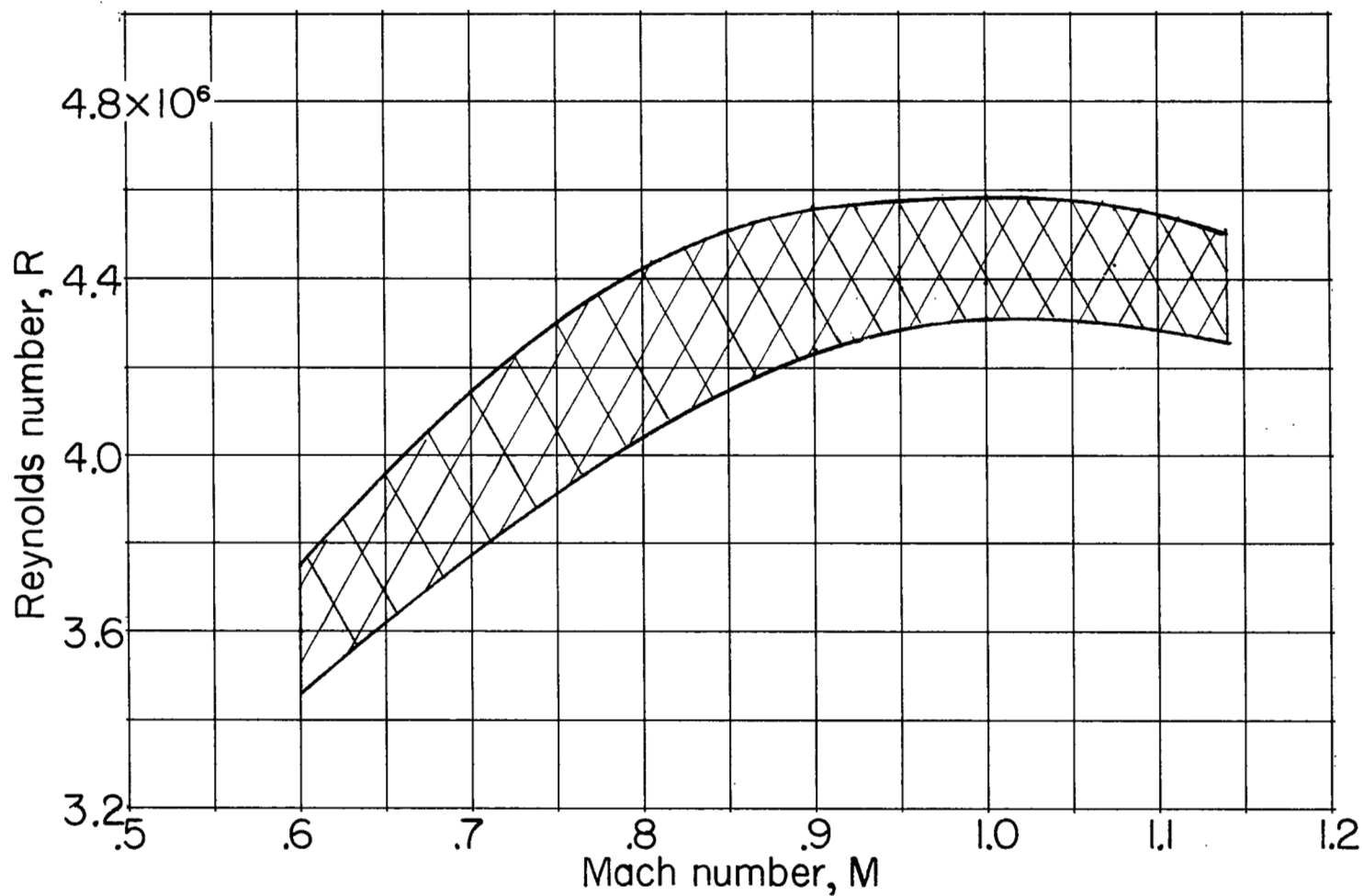


Figure 4.- Variation with Mach number of test Reynolds number based on the various mean aerodynamic chords.

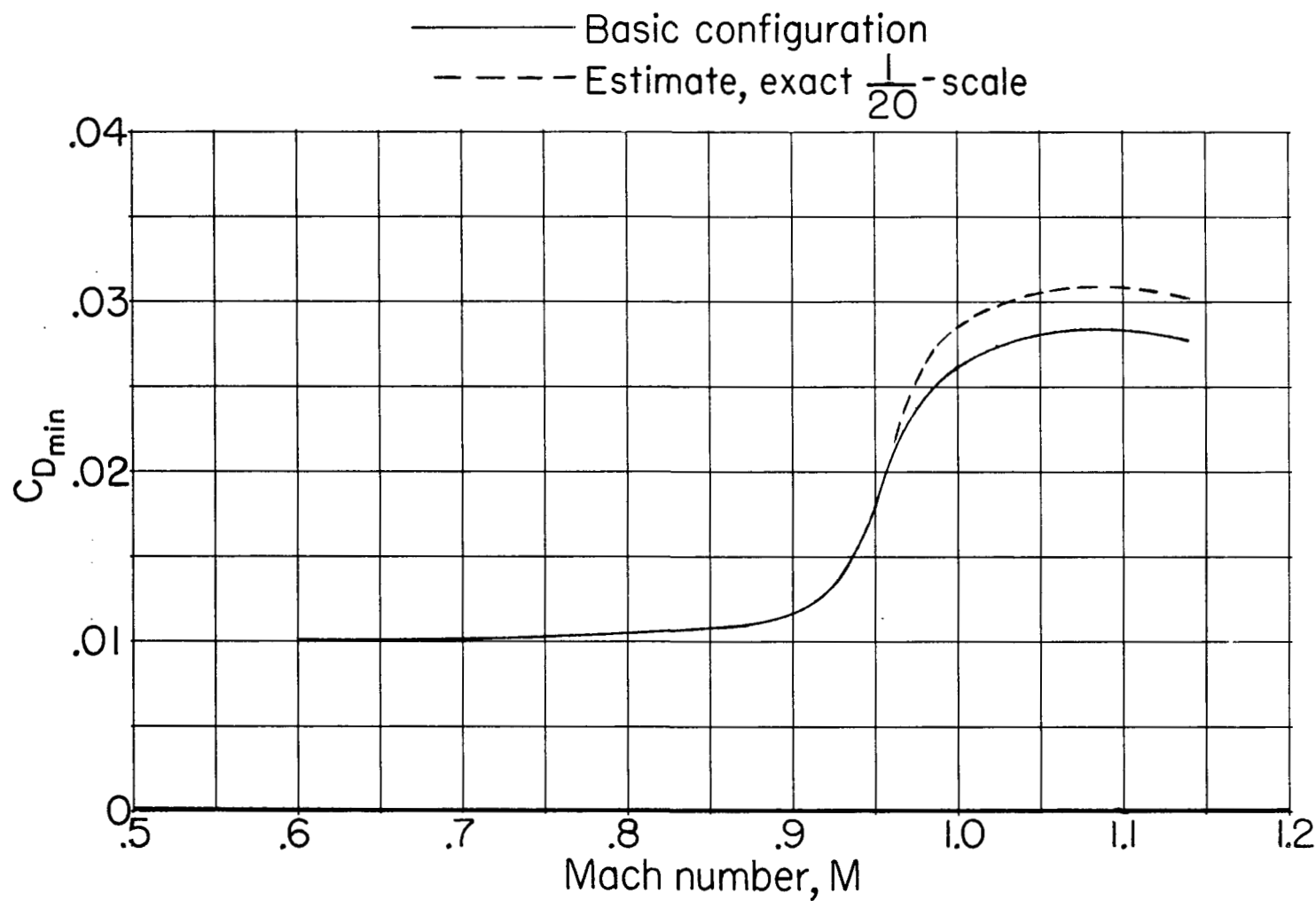


Figure 5.- Comparison of the transonic drag rise of the basic configuration used in the investigation with the estimate for an exact 1/20-scale model.

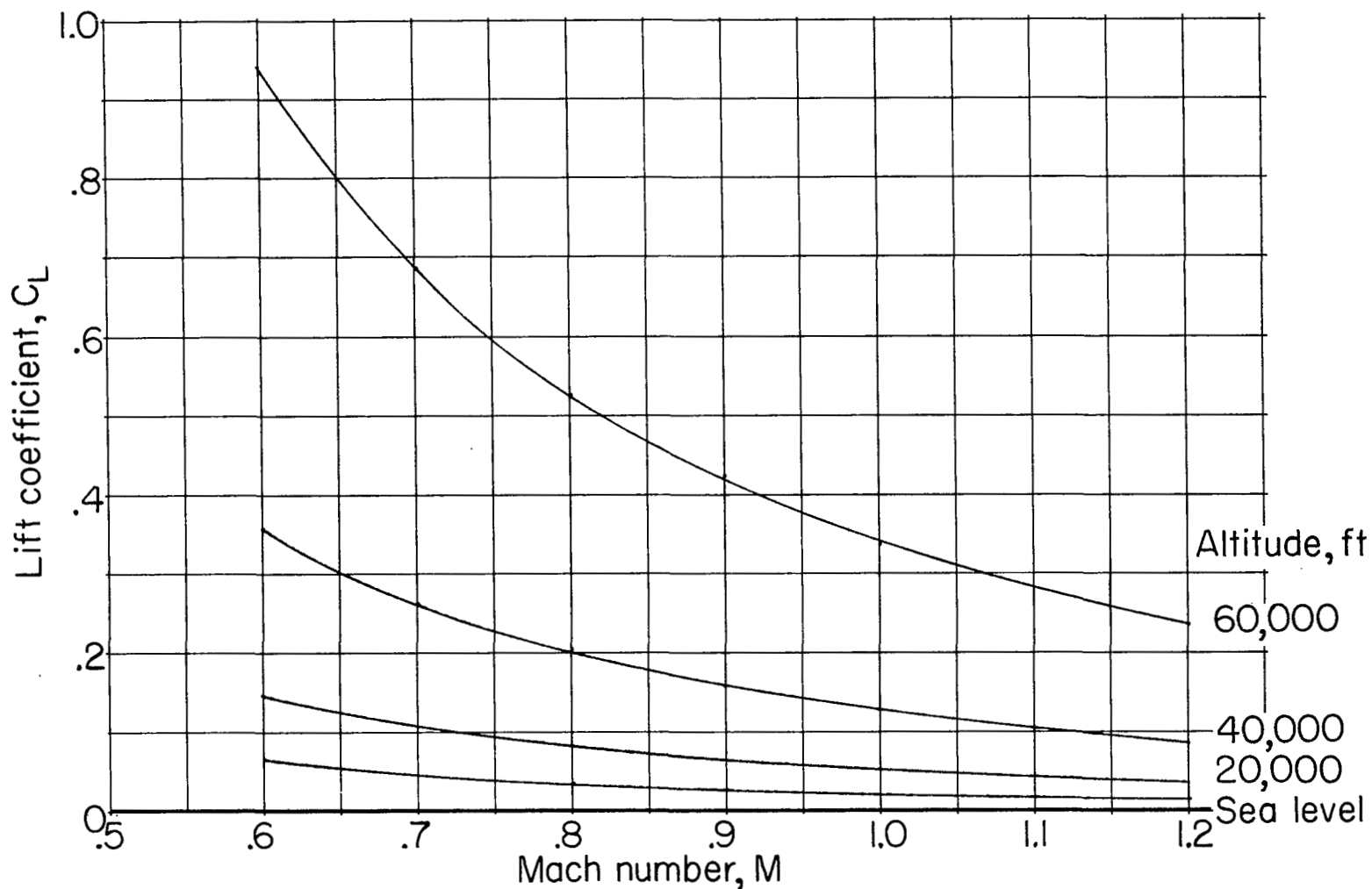


Figure 6.- Variation with Mach number of the lift coefficient required for level flight at several altitudes for a wing loading of 35.4 pounds per square foot.

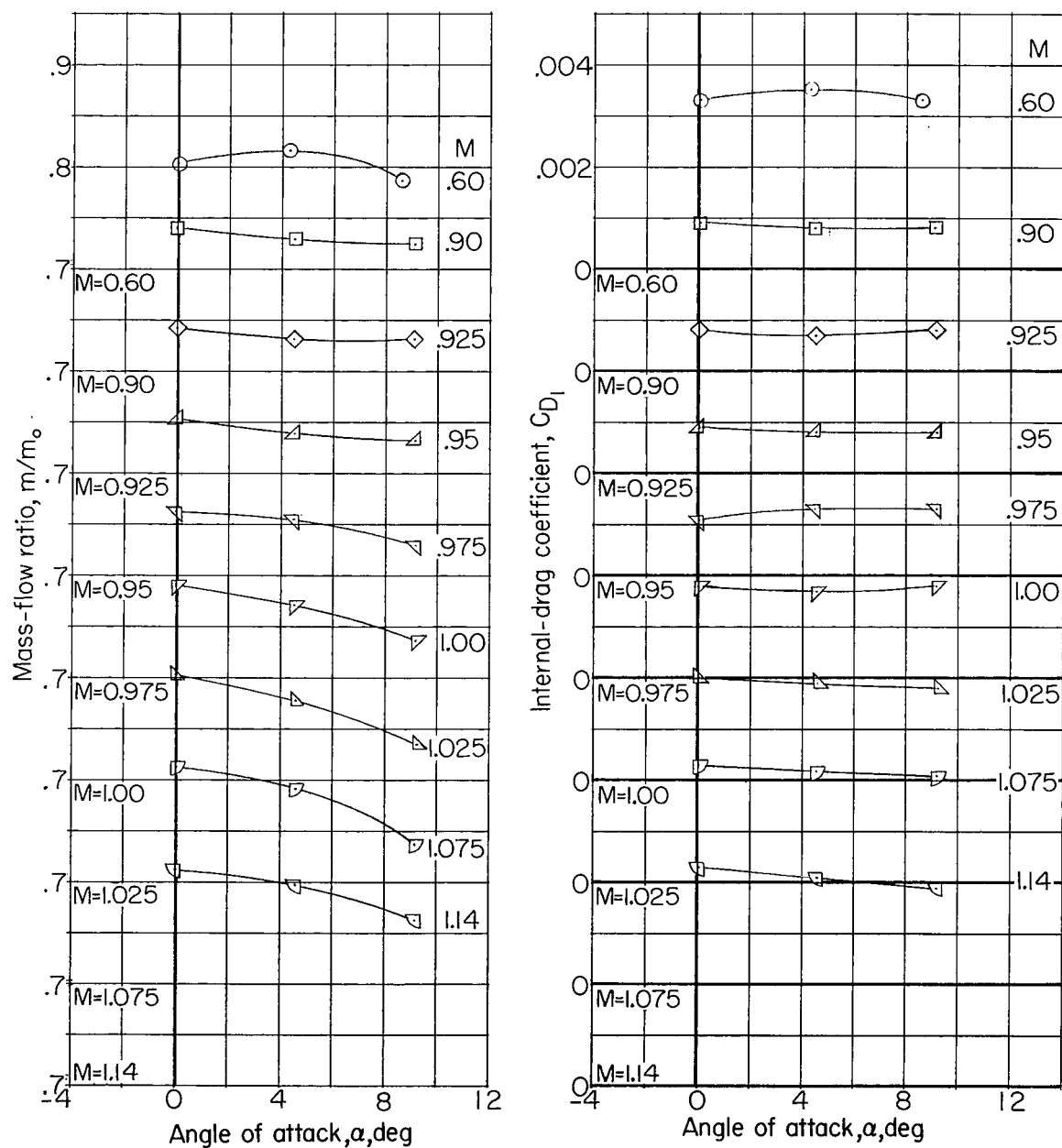
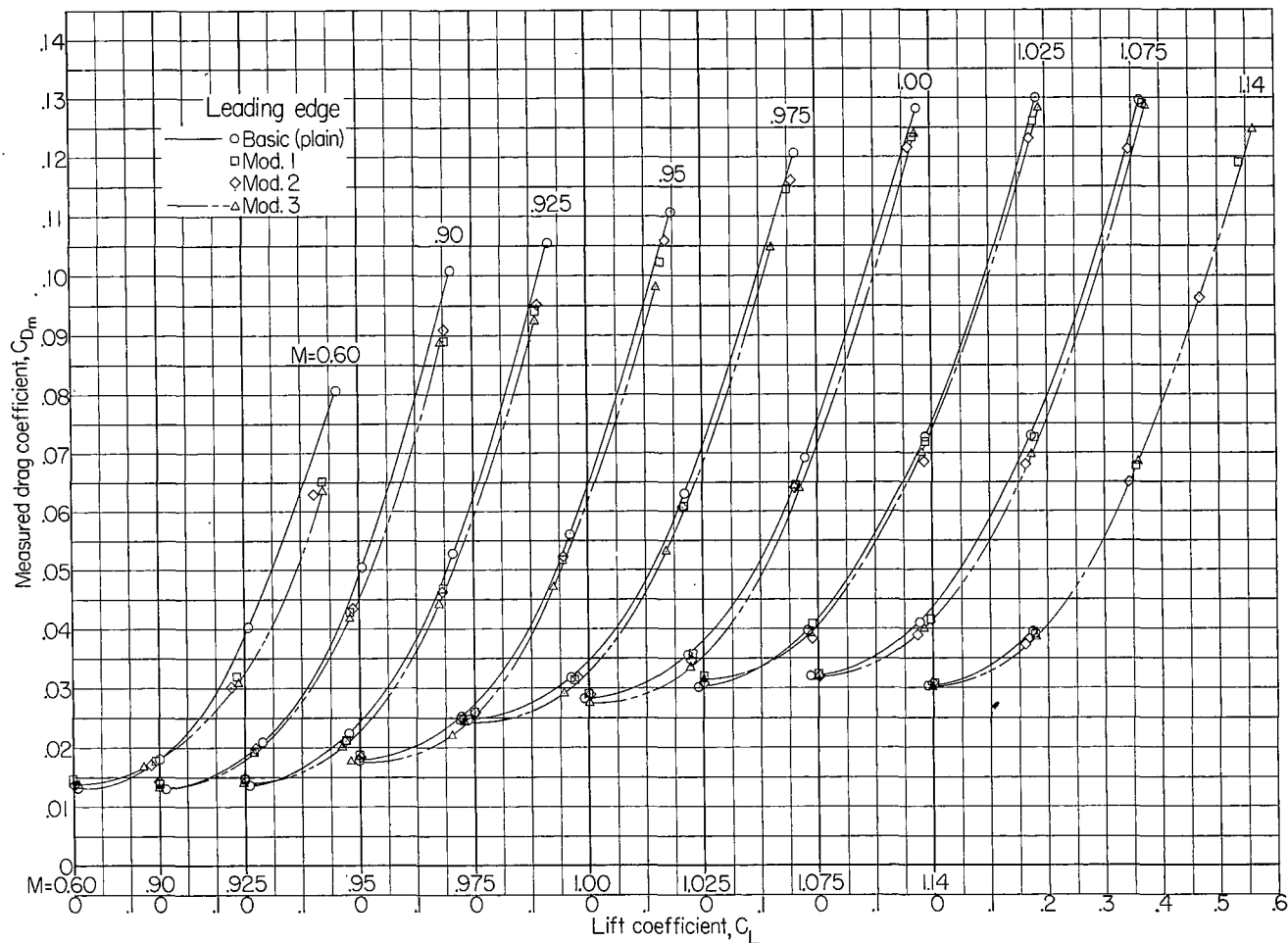
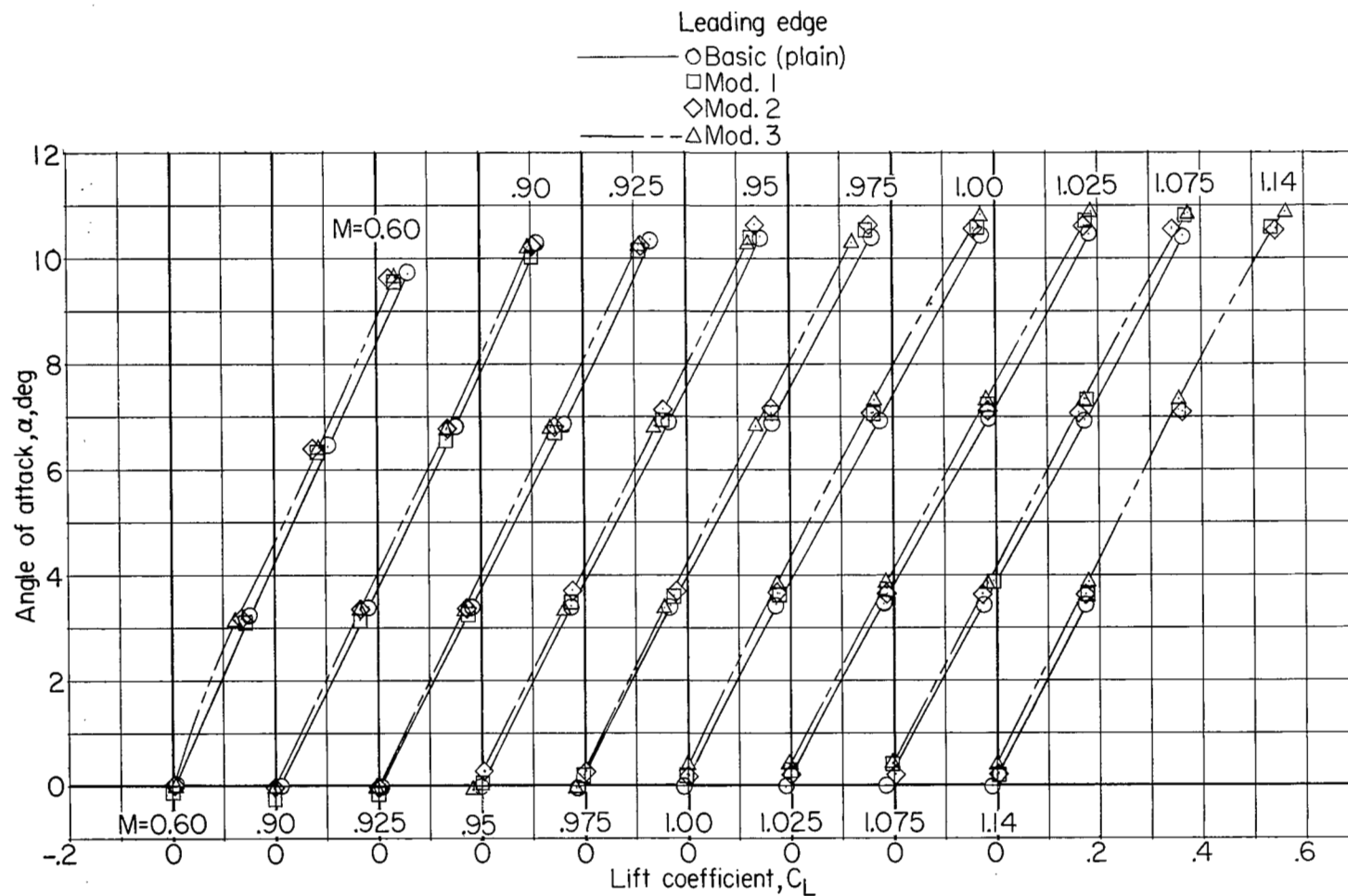


Figure 7.- Mass-flow ratios and internal drag coefficients for the basic configuration with  $0^\circ$  elevator deflection.



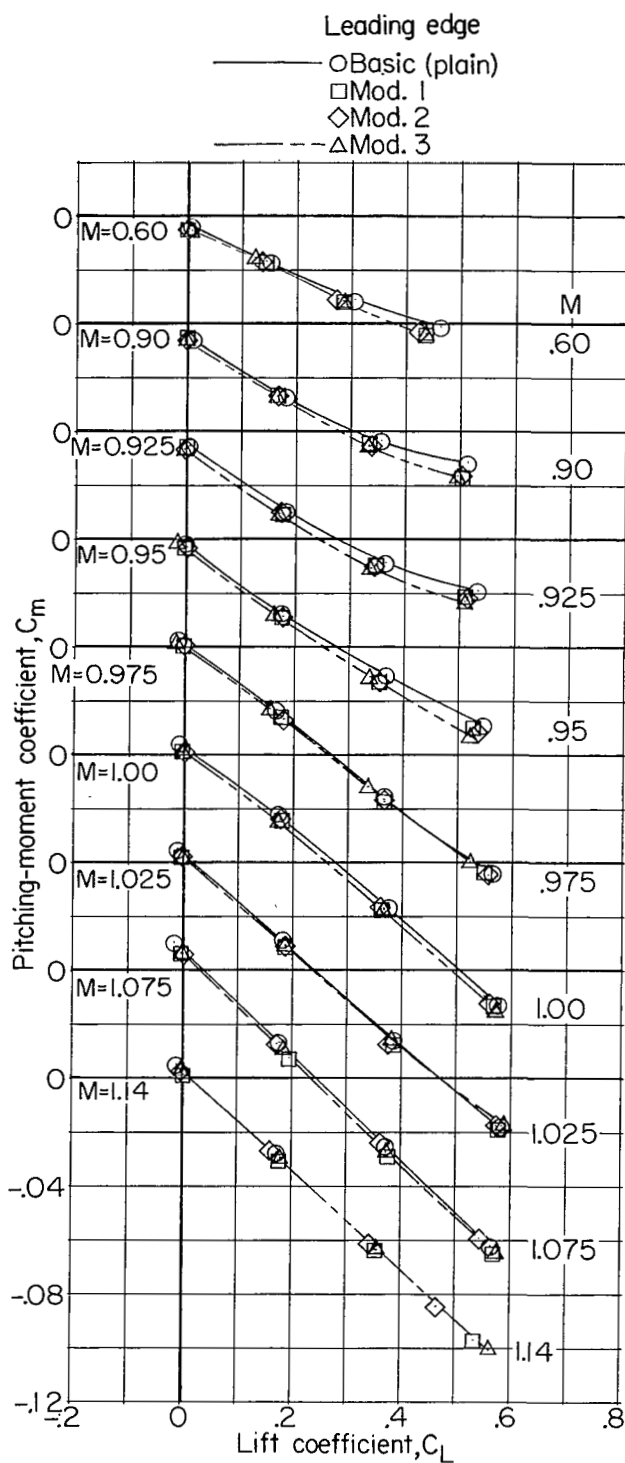
(a) Drag.

Figure 8.- Effects of leading-edge modifications on the force and moment characteristics of the basic configuration. Modifications 1 to 3.



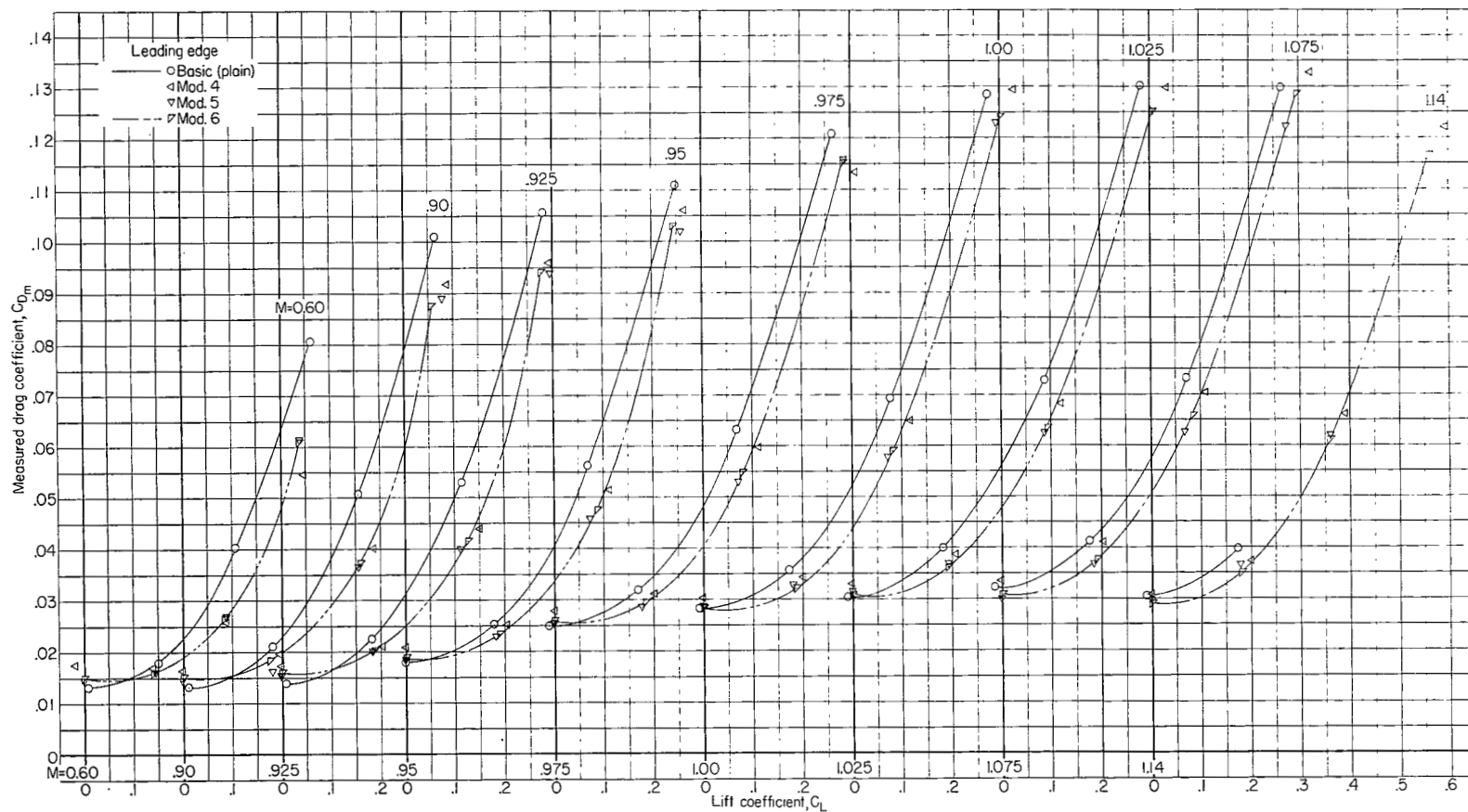
(b) Lift.

Figure 8.- Continued.



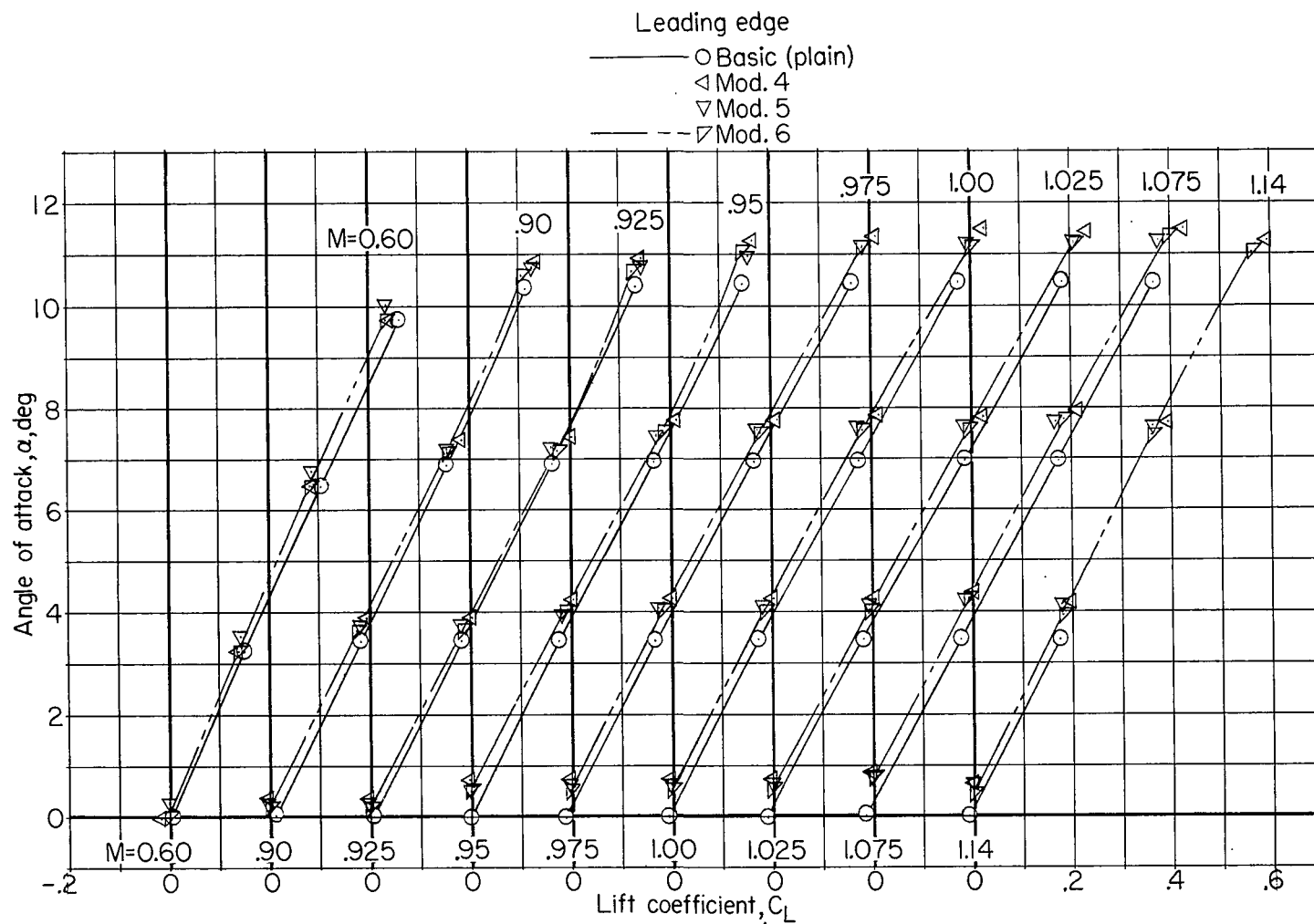
(c) Pitching moment.

Figure 8.- Concluded.



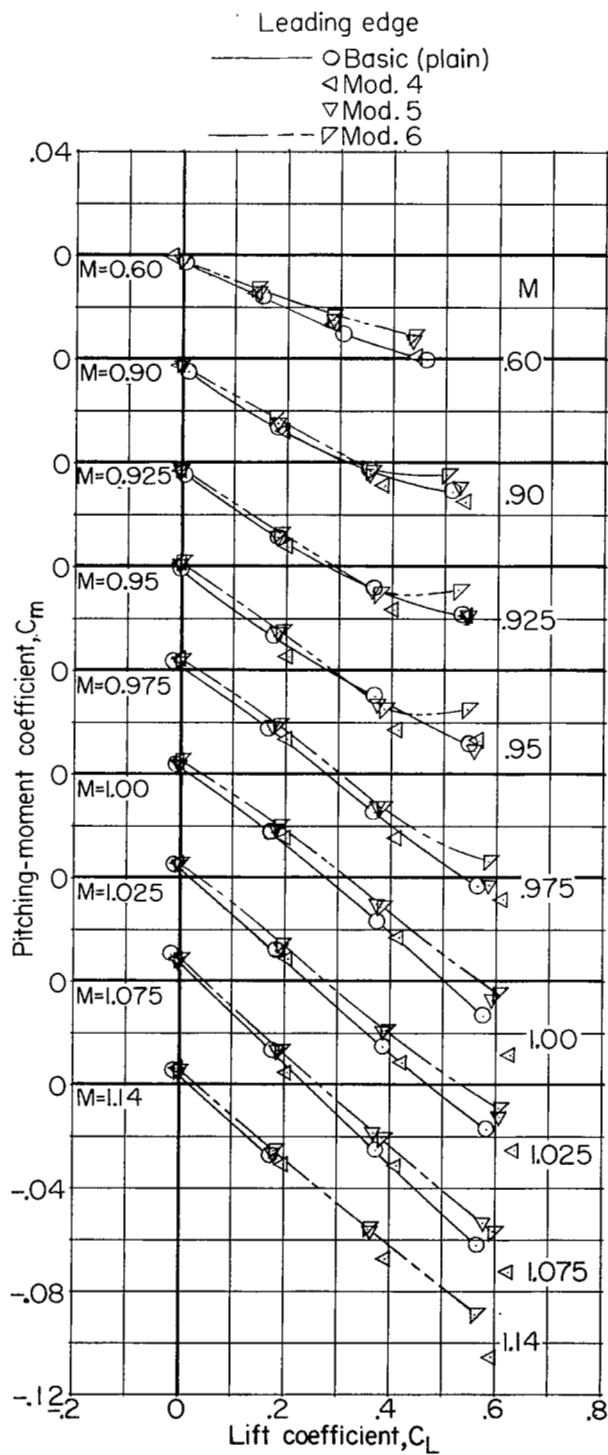
(a) Drag.

Figure 9.- Effects of leading-edge modifications on the force and moment characteristics of the basic configuration. Modifications 4 to 6.



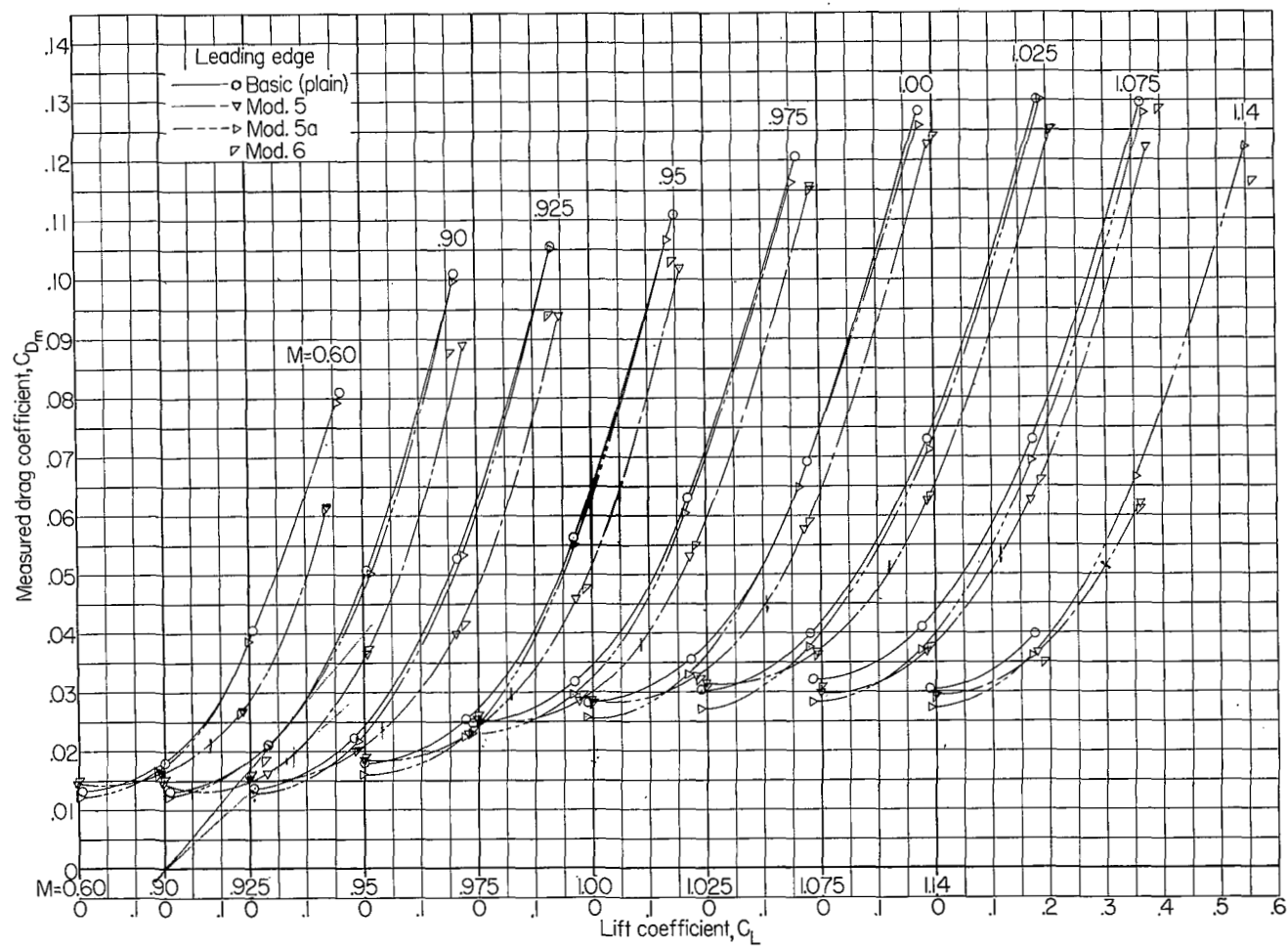
(b) Lift.

Figure 9.- Continued.



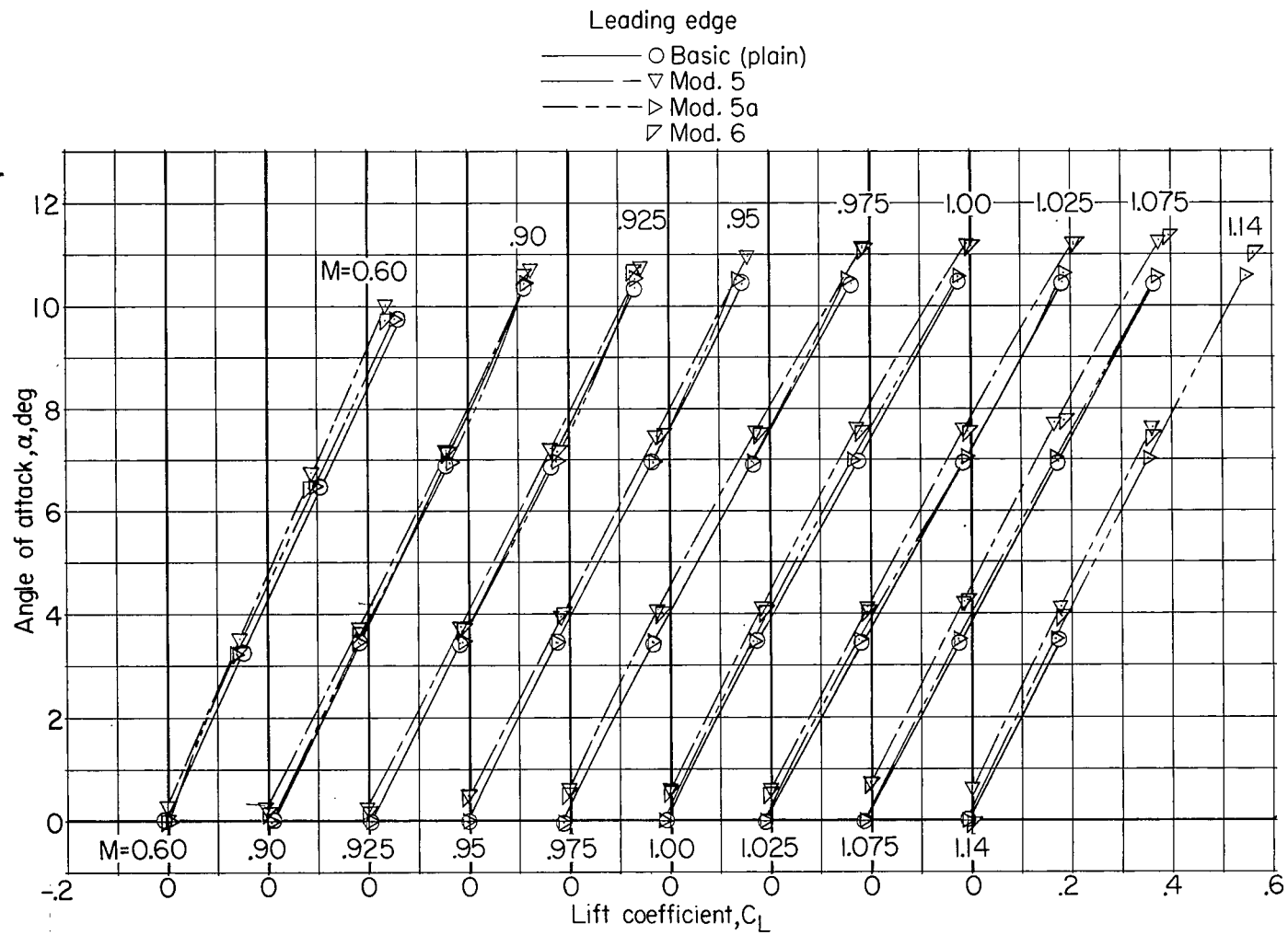
(c) Pitching moment.

Figure 9.- Concluded.



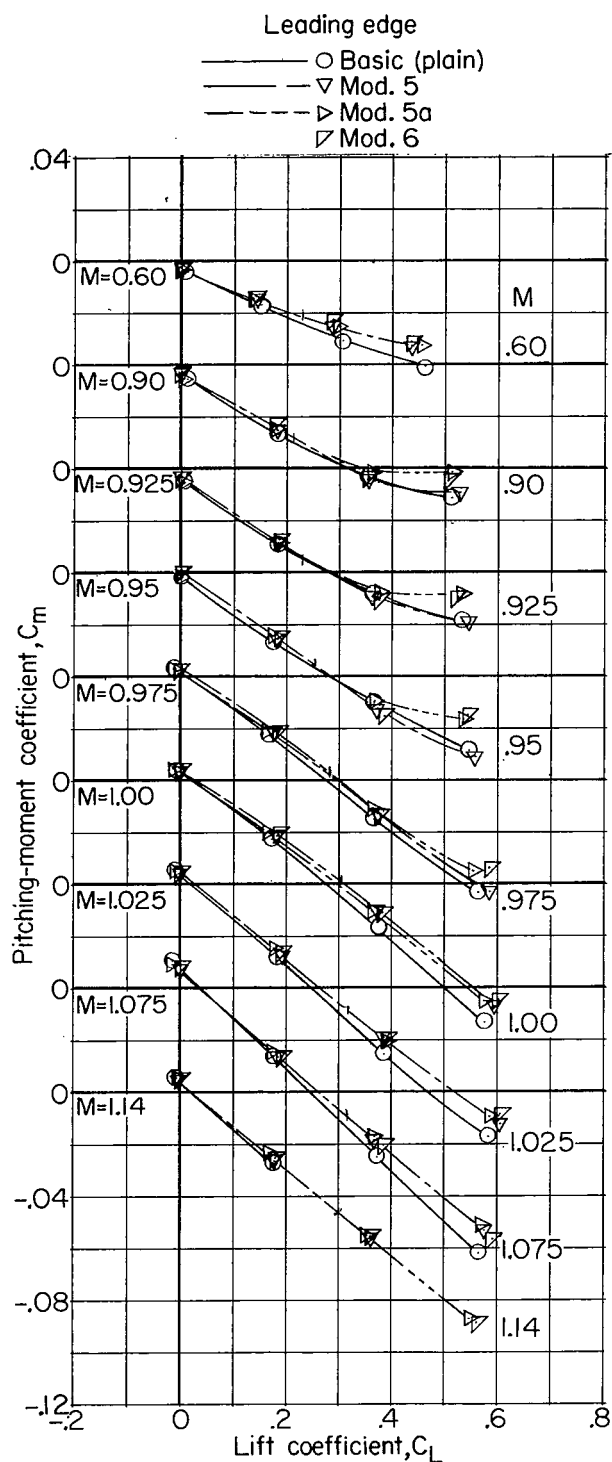
(a) Drag.

Figure 10.- Effects of plan form change on the force and moment characteristics of the basic configuration.



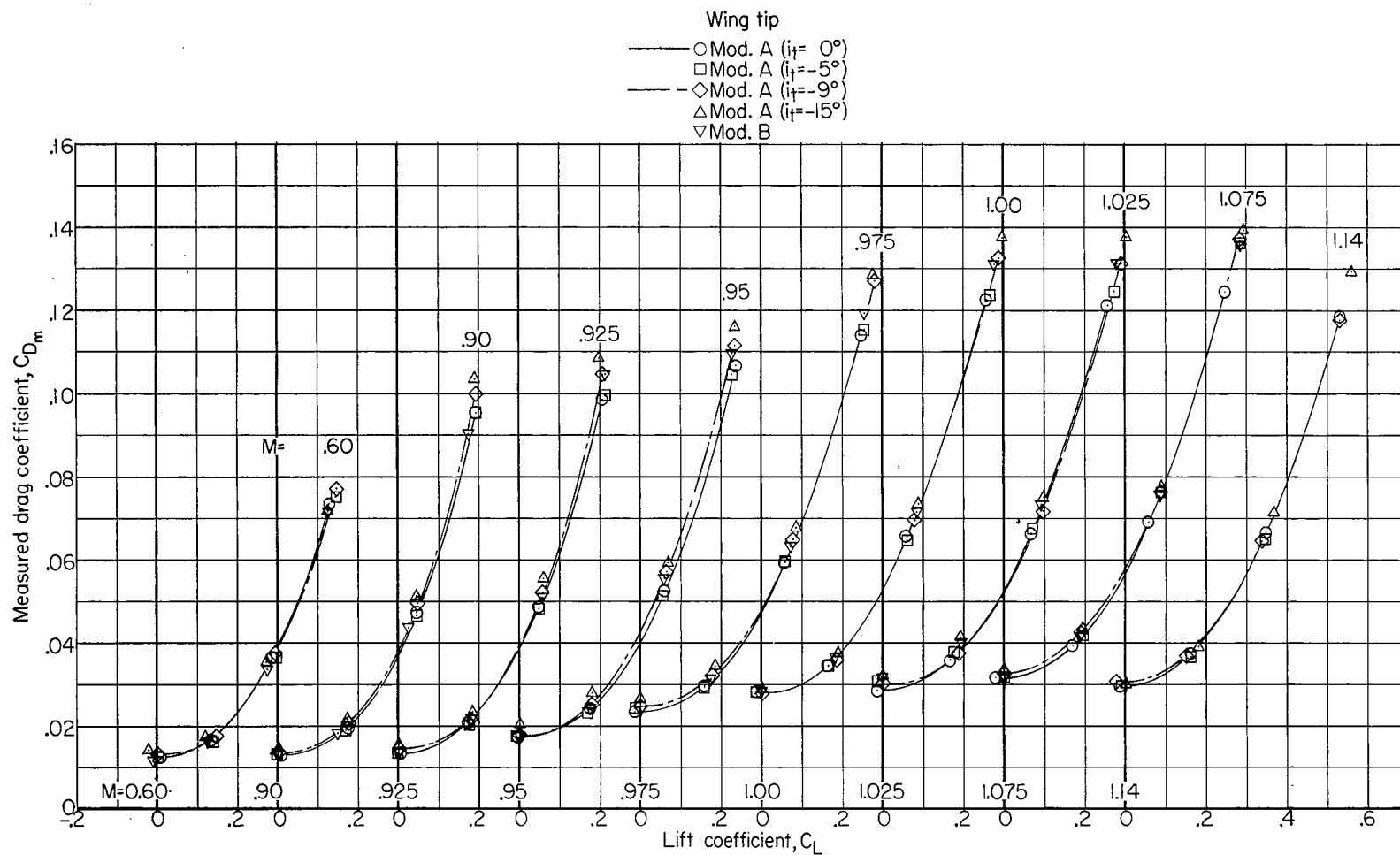
(b) Lift.

Figure 10.- Continued.



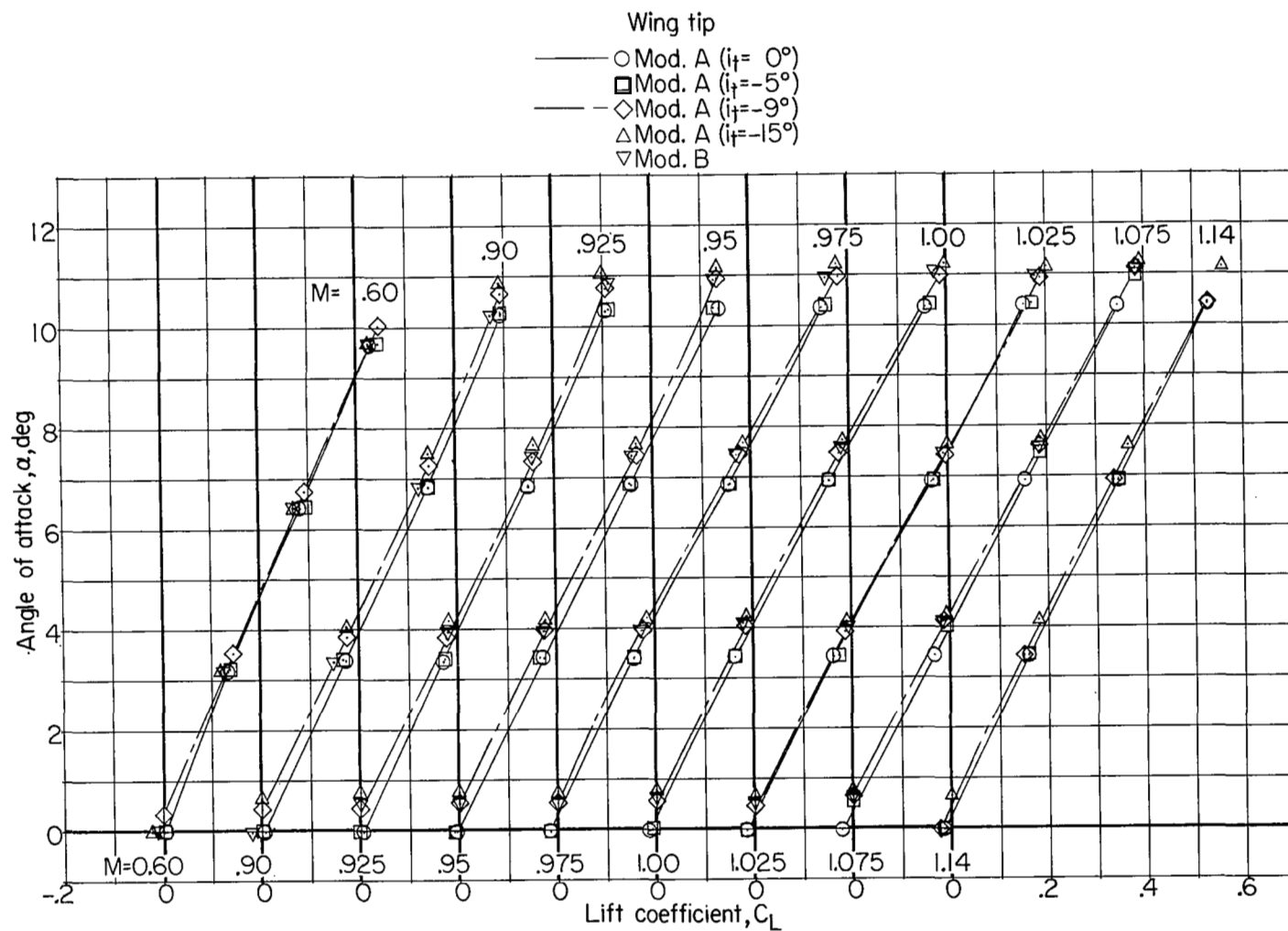
(c) Pitching moment.

Figure 10.- Concluded.



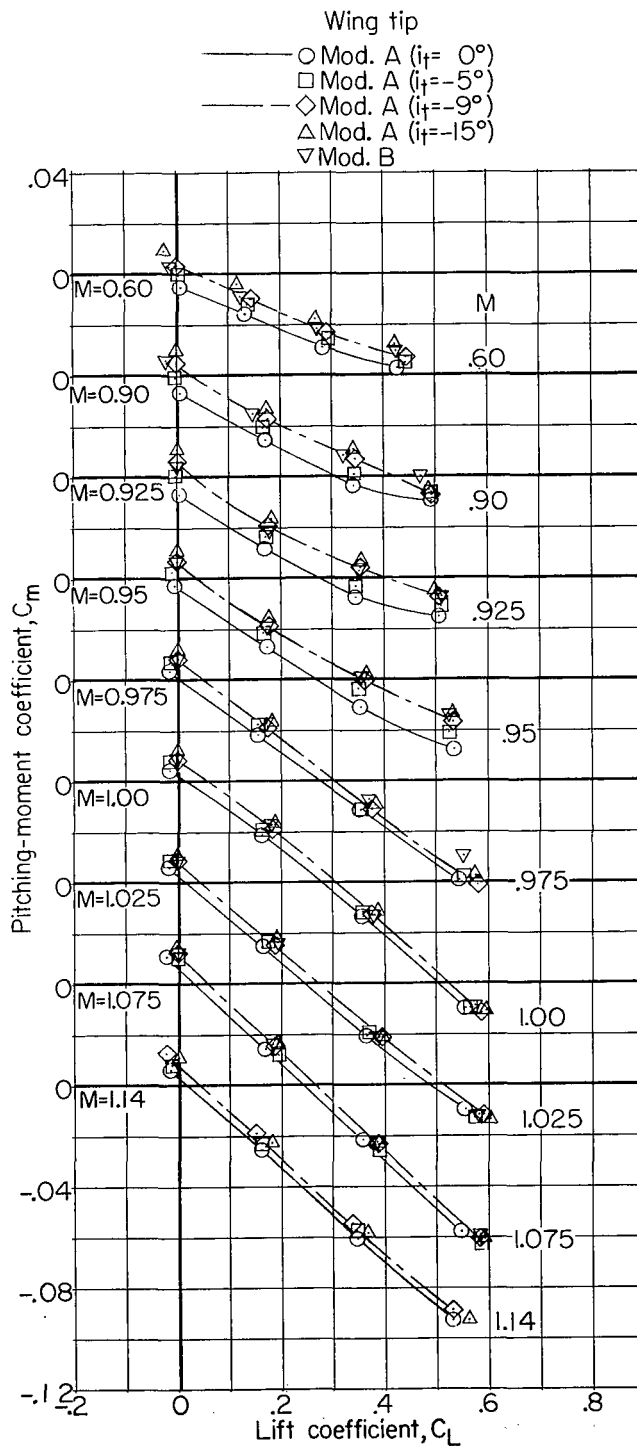
(a) Drag.

Figure 11.- Force and moment characteristics of the wing-tip modifications.



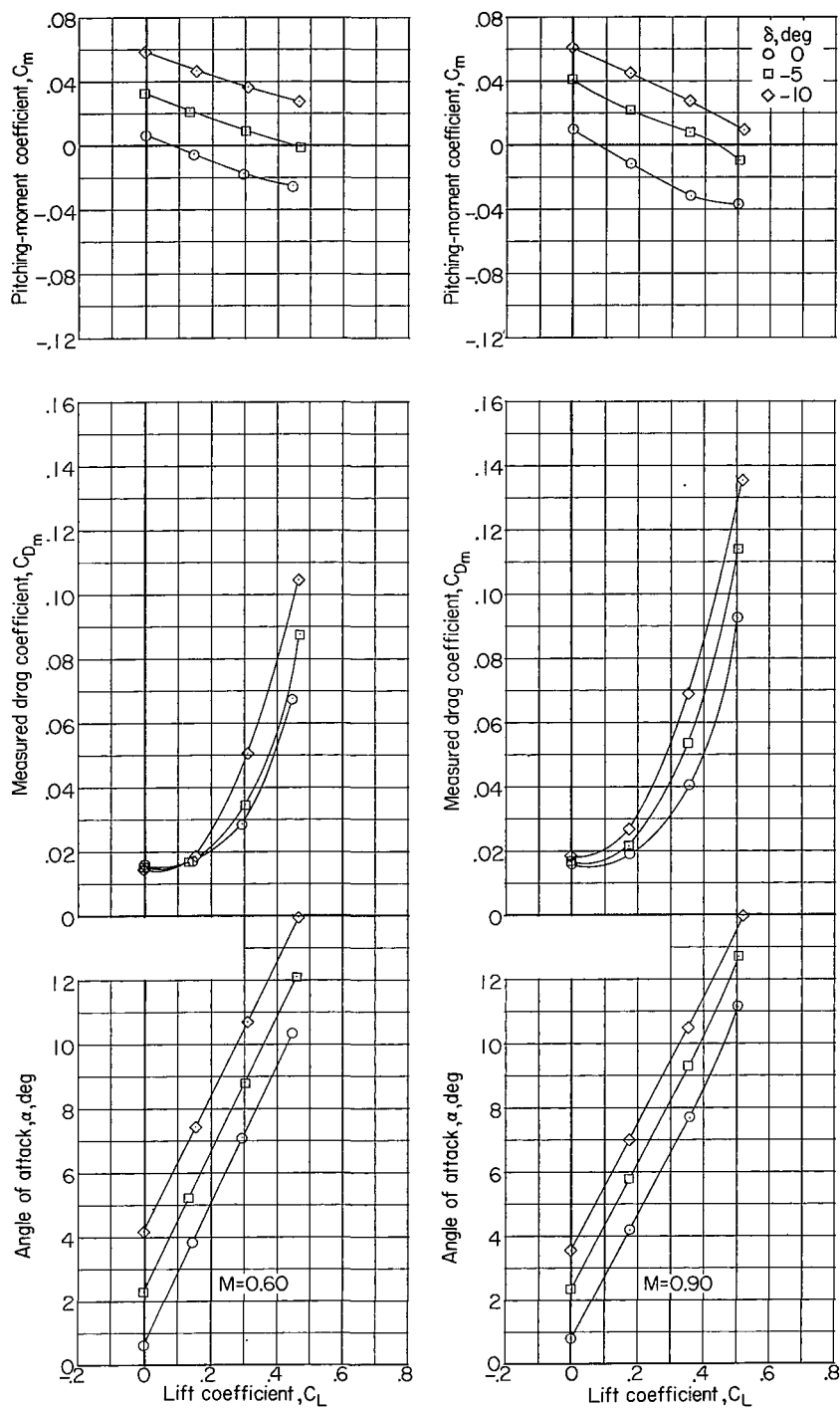
(b) Lift.

Figure 11.- Continued.



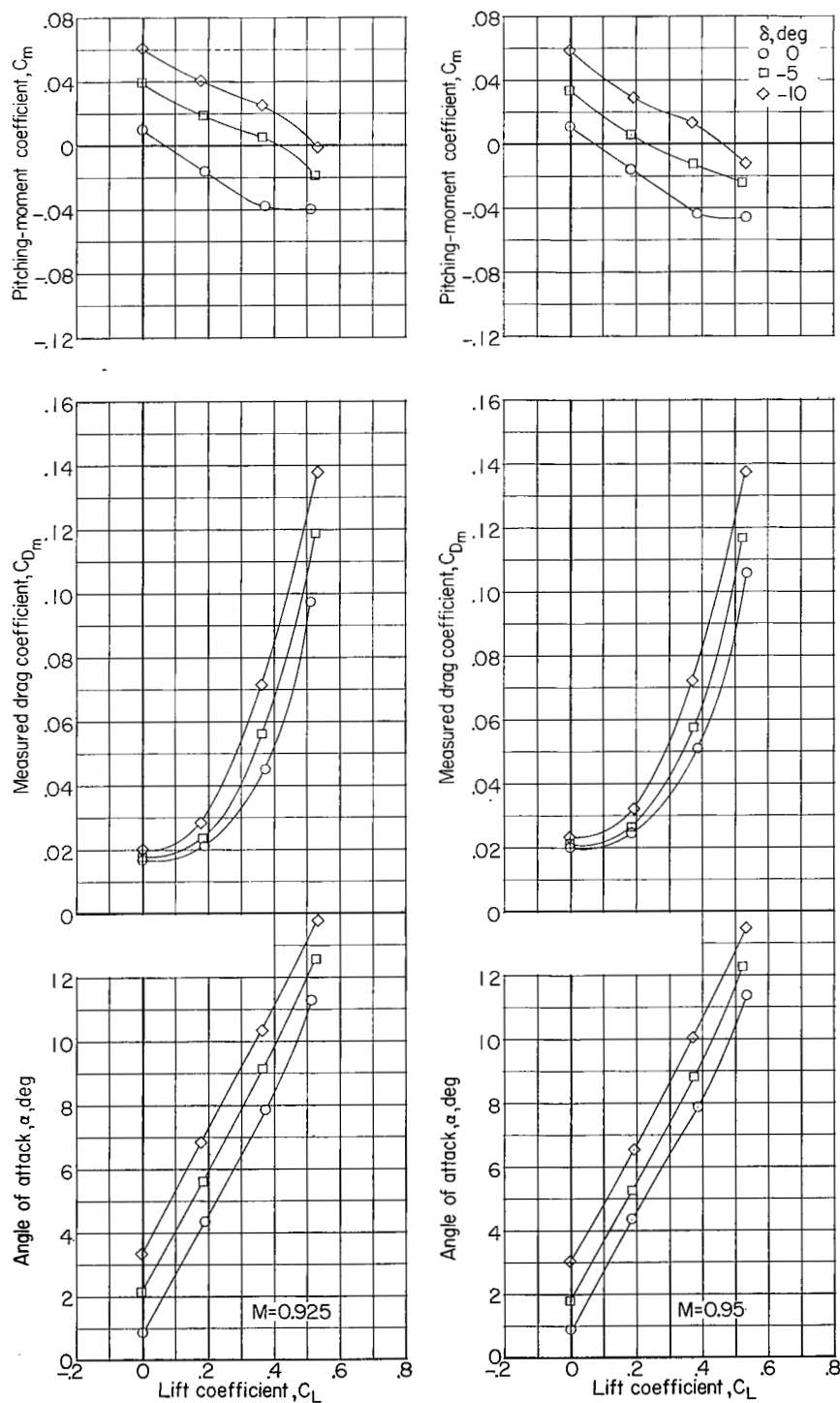
(c) Pitching moment.

Figure 11.- Concluded.



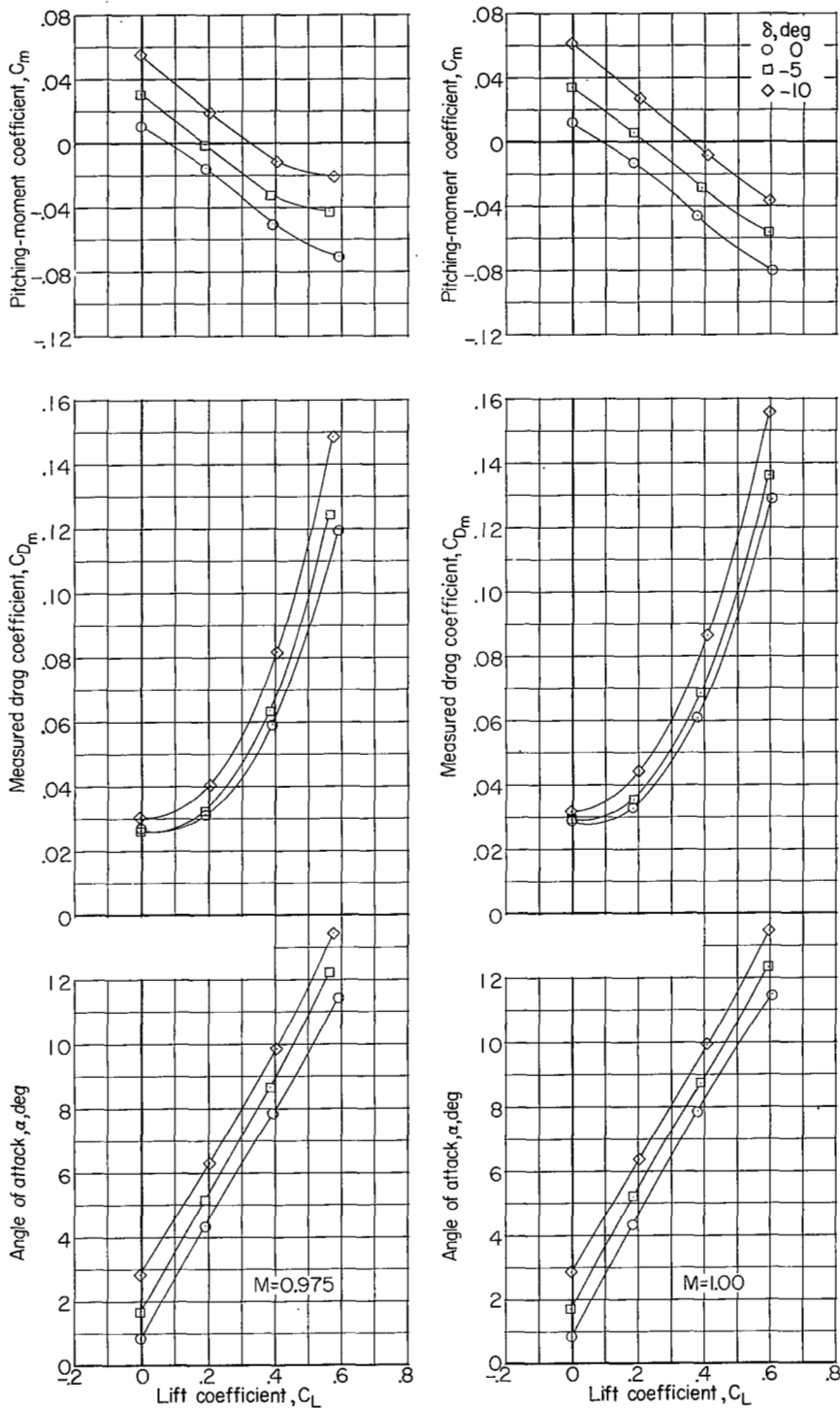
(a)  $M = 0.60$  and  $0.90$ .

Figure 12.- Force and moment characteristics of the modified wing model with various elevator deflections.



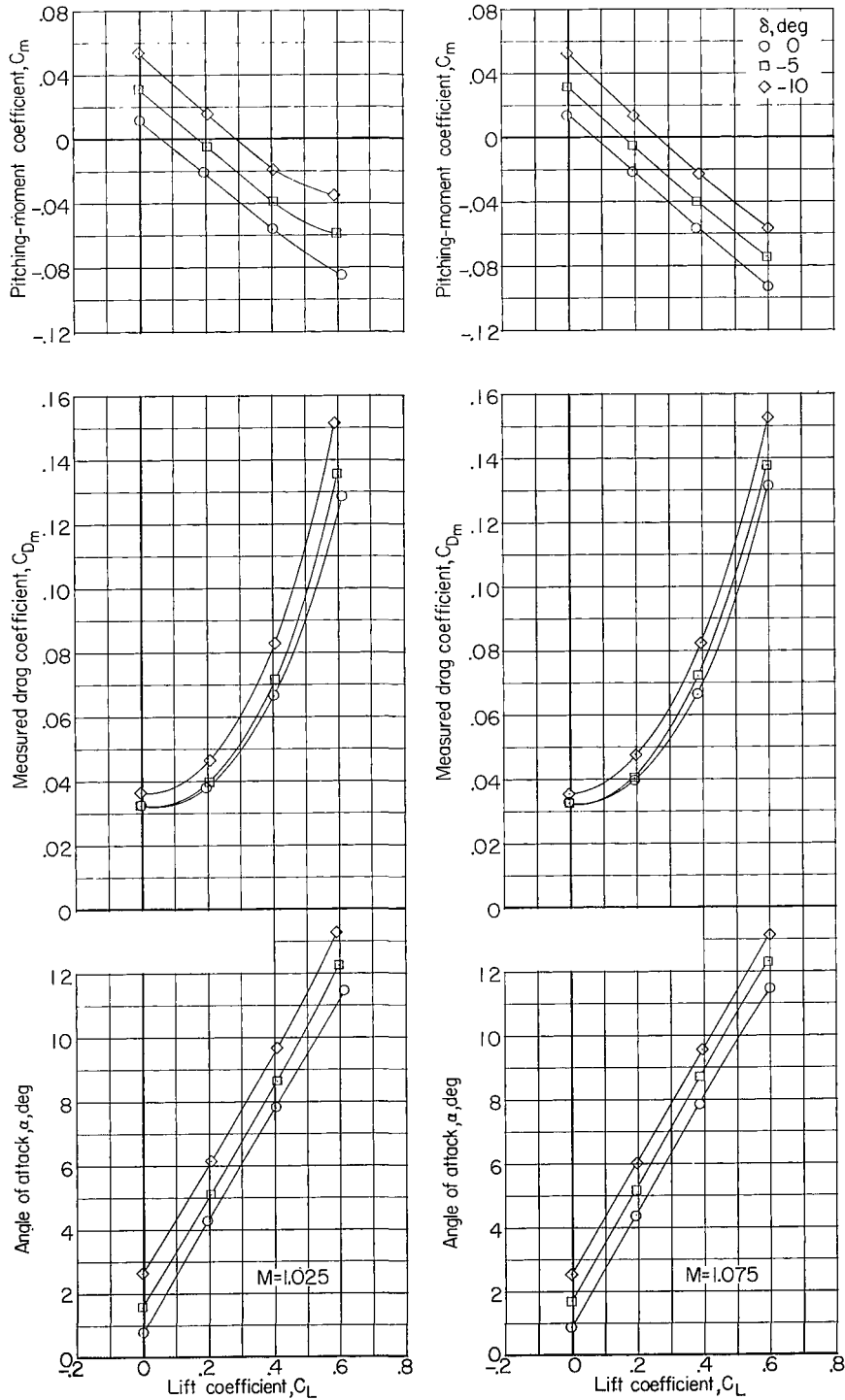
(b)  $M = 0.925$  and  $0.95$ .

Figure 12.- Continued.



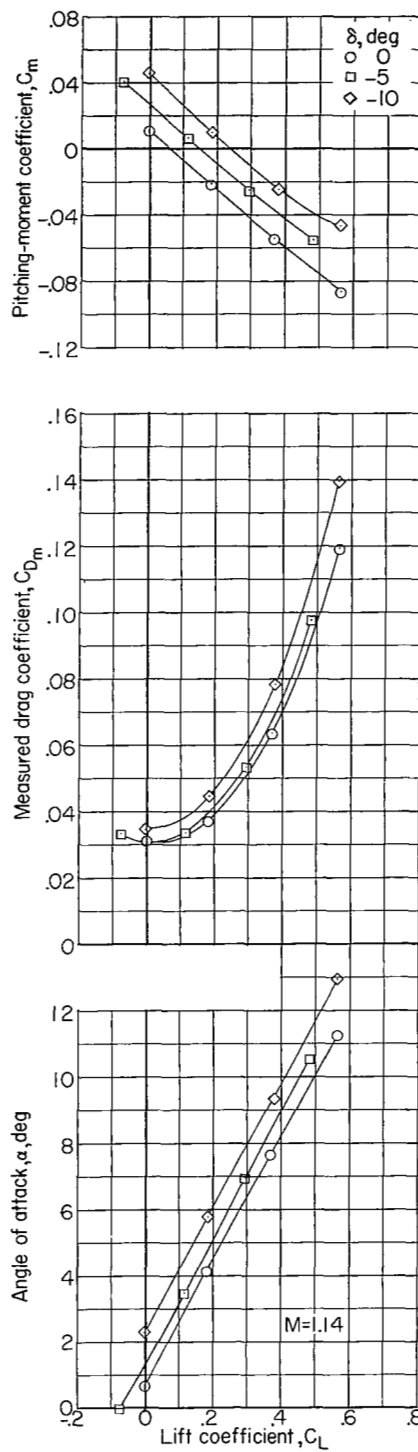
(c)  $M = 0.975$  and  $1.00$ .

Figure 12.- Continued.



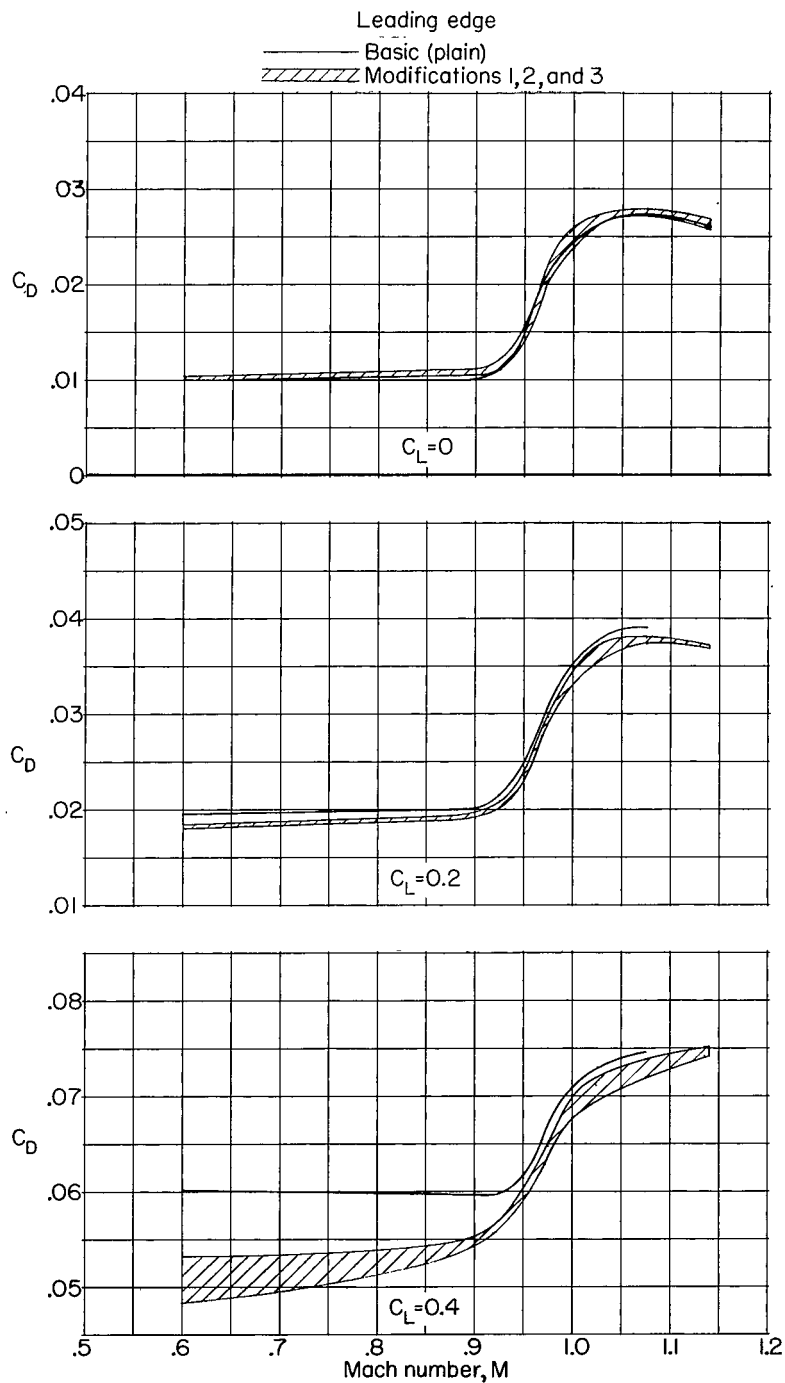
(d)  $M = 1.025$  and  $1.075$ .

Figure 12.- Continued.



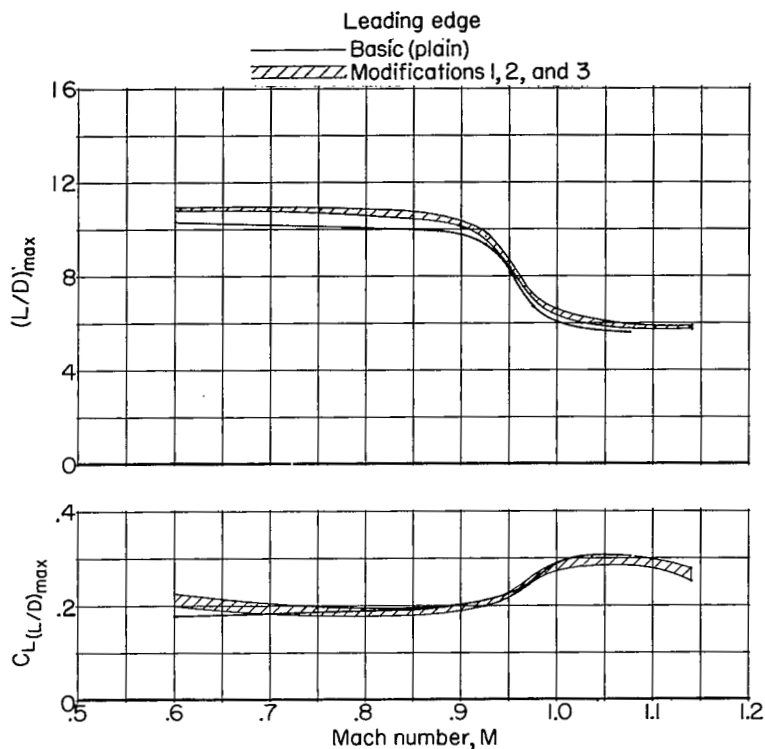
(e)  $M = 1.140$ .

Figure 12.- Concluded.

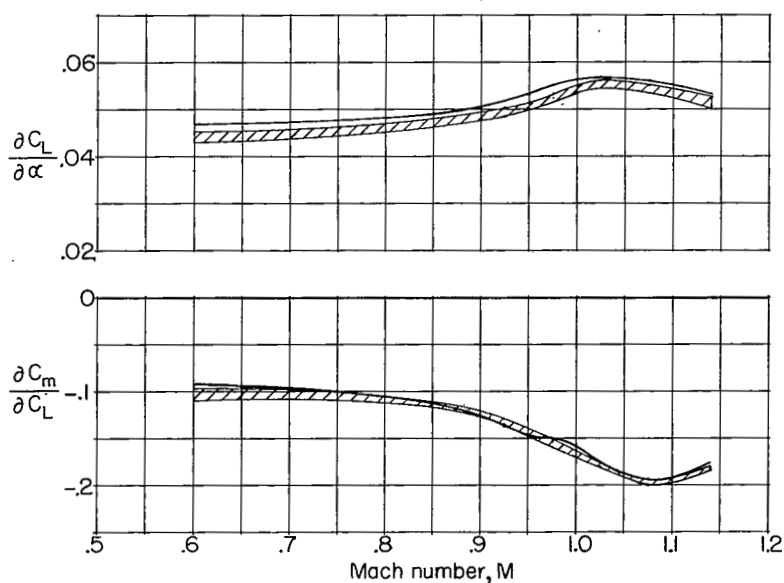


(a) Drag characteristics at several lift coefficients.

Figure 13.- Effects of leading-edge modifications 1, 2, and 3 on aerodynamic parameters of the basic configuration. Internal drag removed.

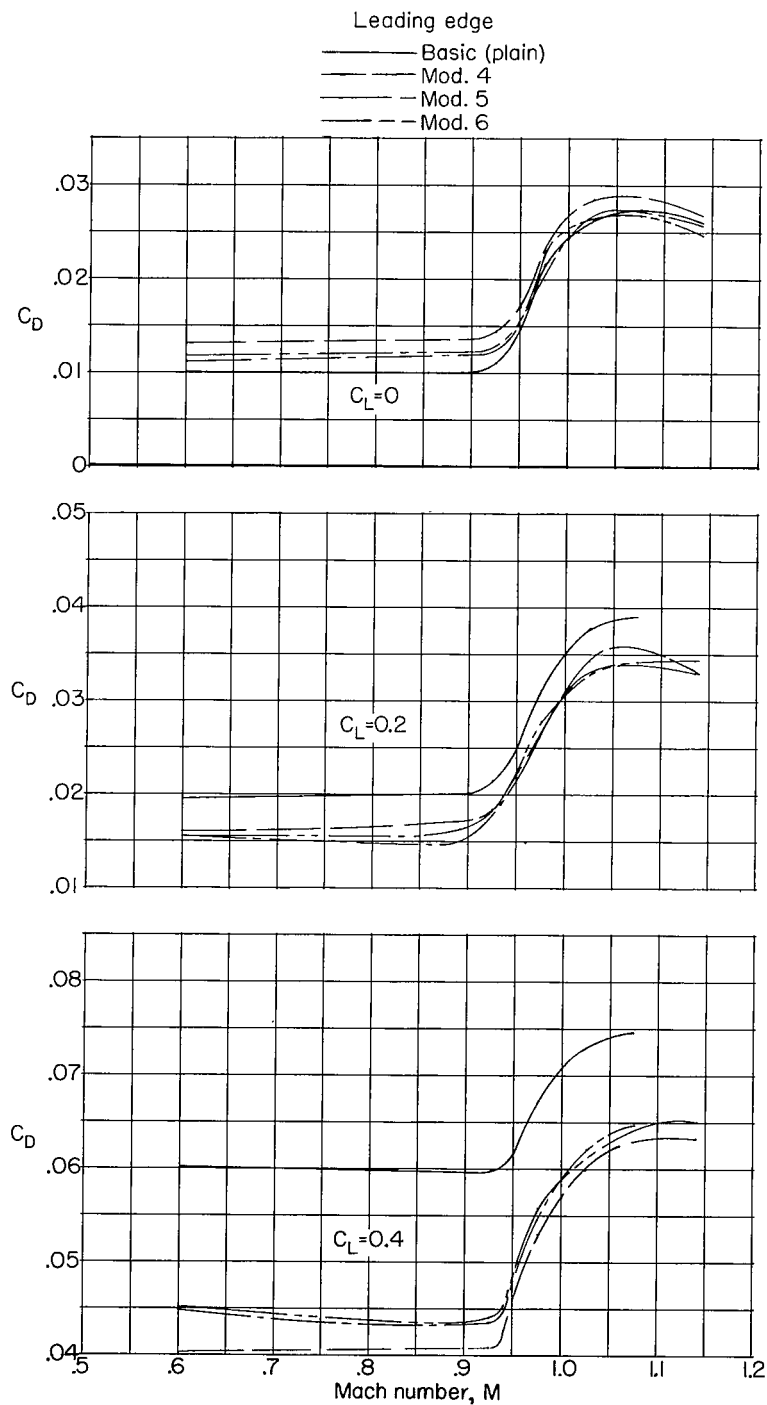


(b) Maximum lift-drag ratio characteristics.



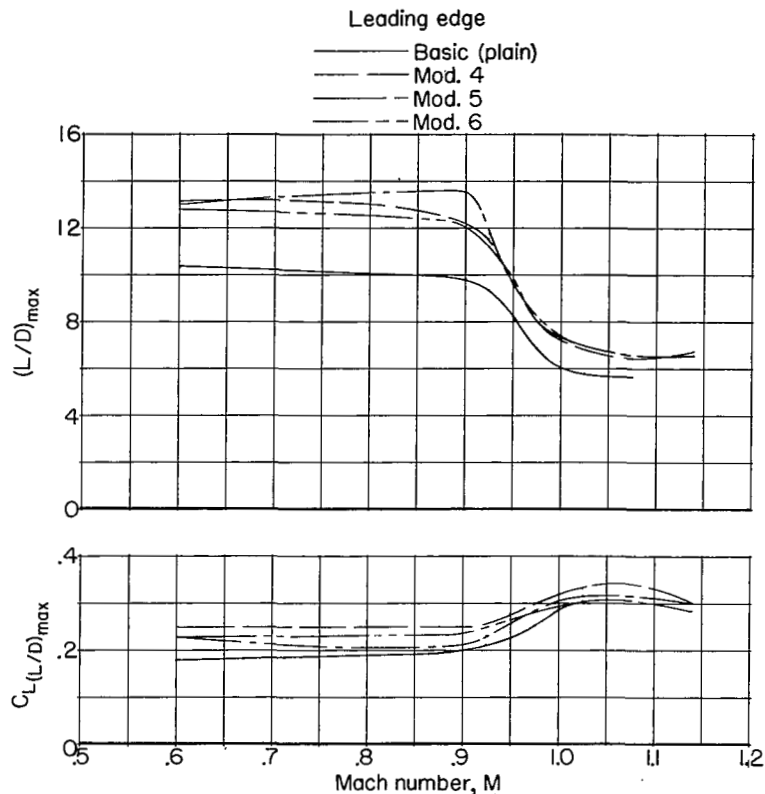
(c) Lift-curve slope and static longitudinal stability.

Figure 13.- Concluded.

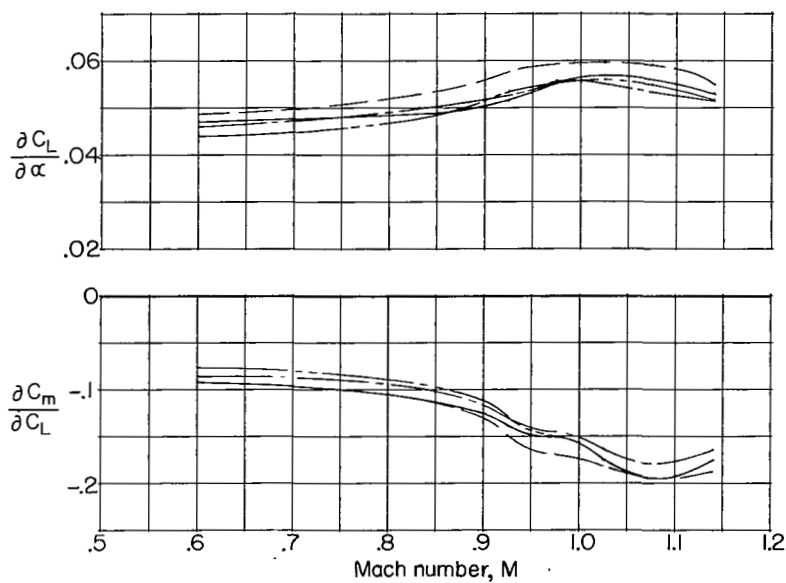


(a) Drag characteristics at several lift coefficients.

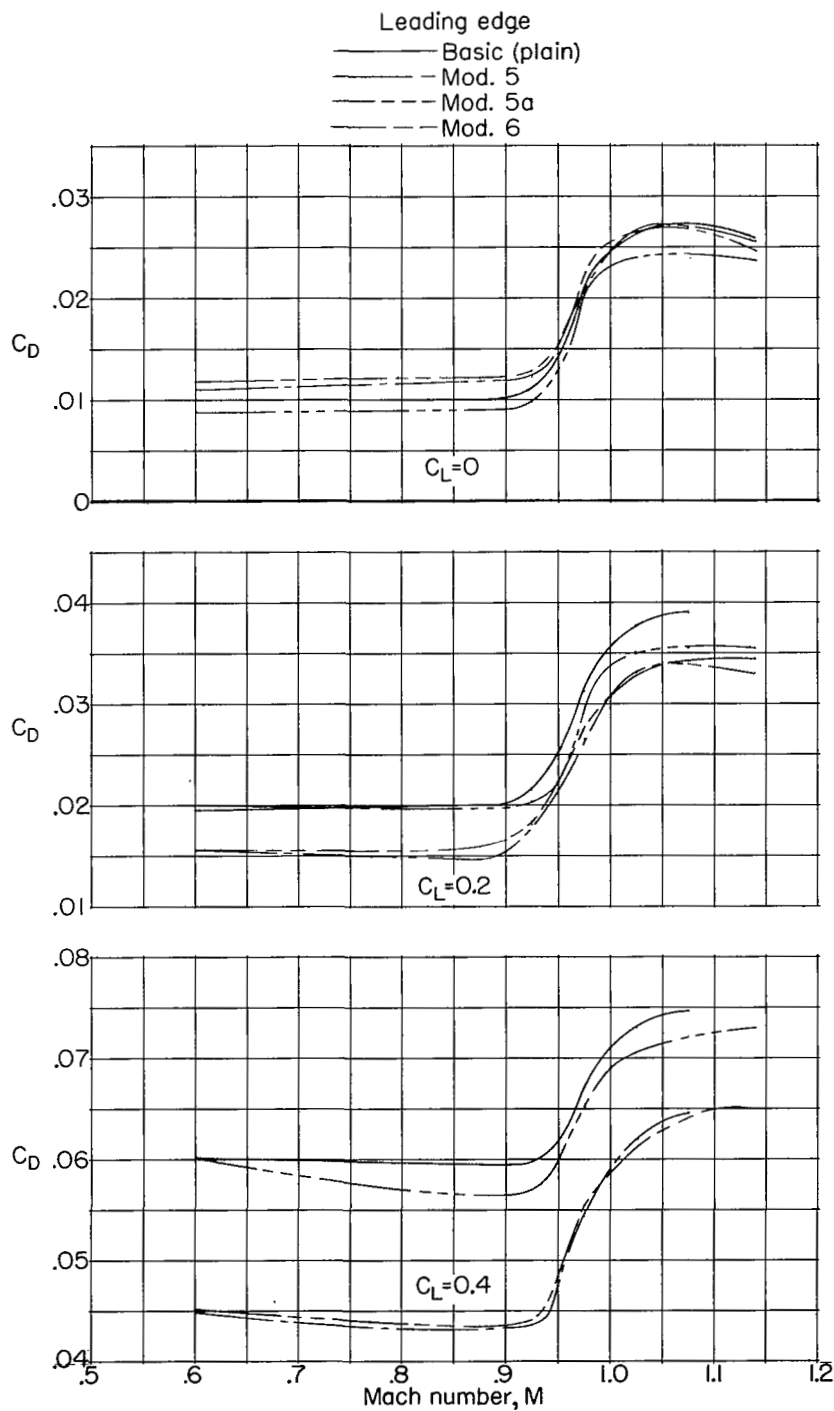
Figure 14.- Effects of leading-edge modifications 4, 5, and 6 on aerodynamic parameters of the basic configuration. Internal drag removed.



(b) Maximum lift-drag ratio characteristics.

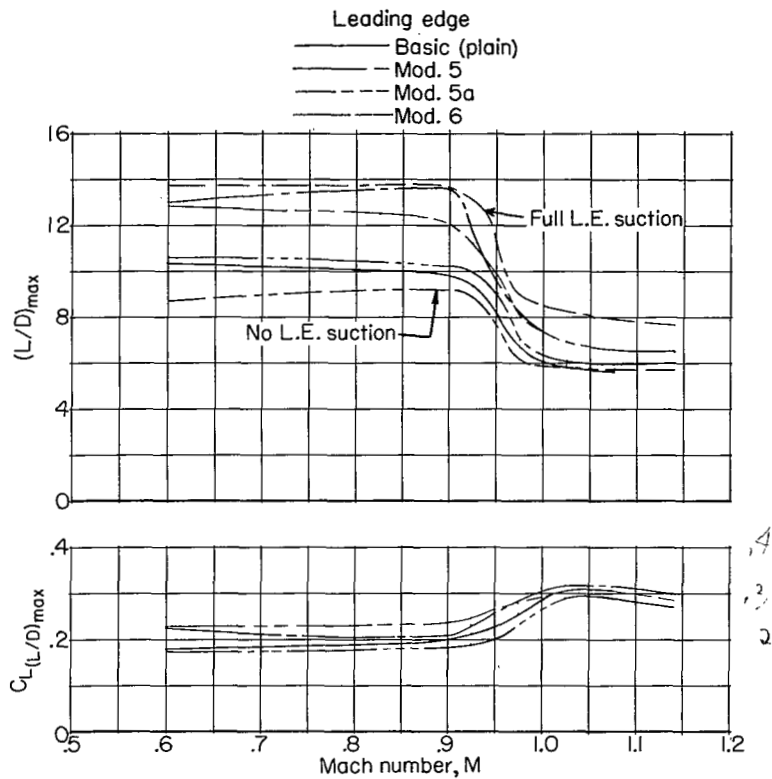


(c) Lift-curve slope and static longitudinal stability.

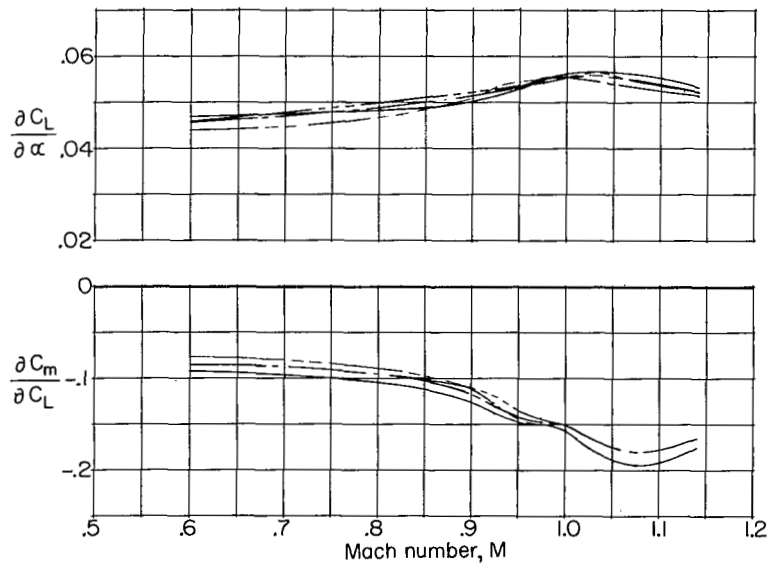


(a) Drag characteristics at several lift coefficients.

Figure 15.- Effects of plan-form change on aerodynamic parameters of the basic configuration. Internal drag removed.



(b) Maximum lift-drag ratio characteristics.



(c) Lift-curve slope and static longitudinal stability.

Figure 15.- Concluded.

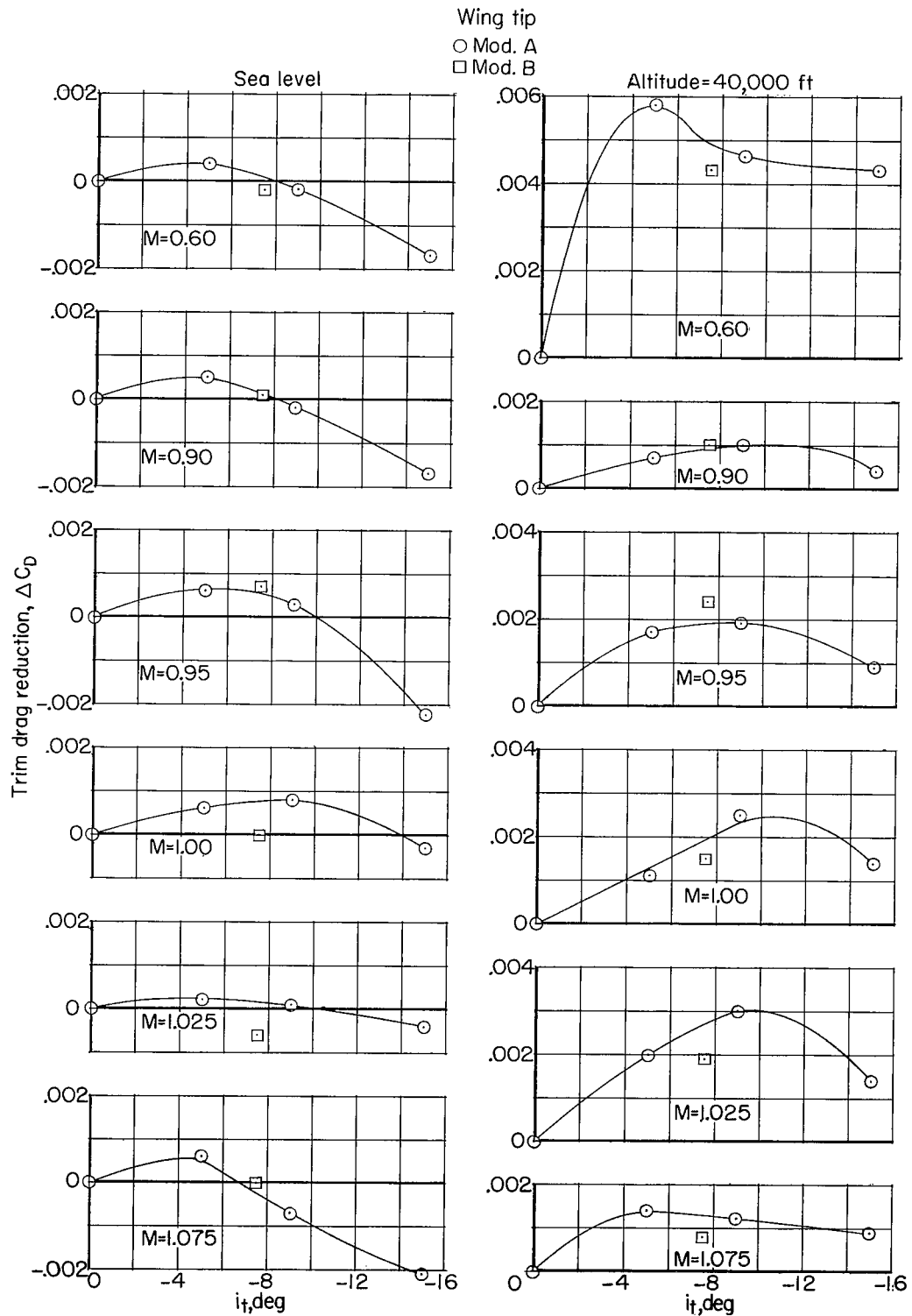


Figure 16.- Variation with tip deflection of the trim drag reduction for the tip modifications tested.

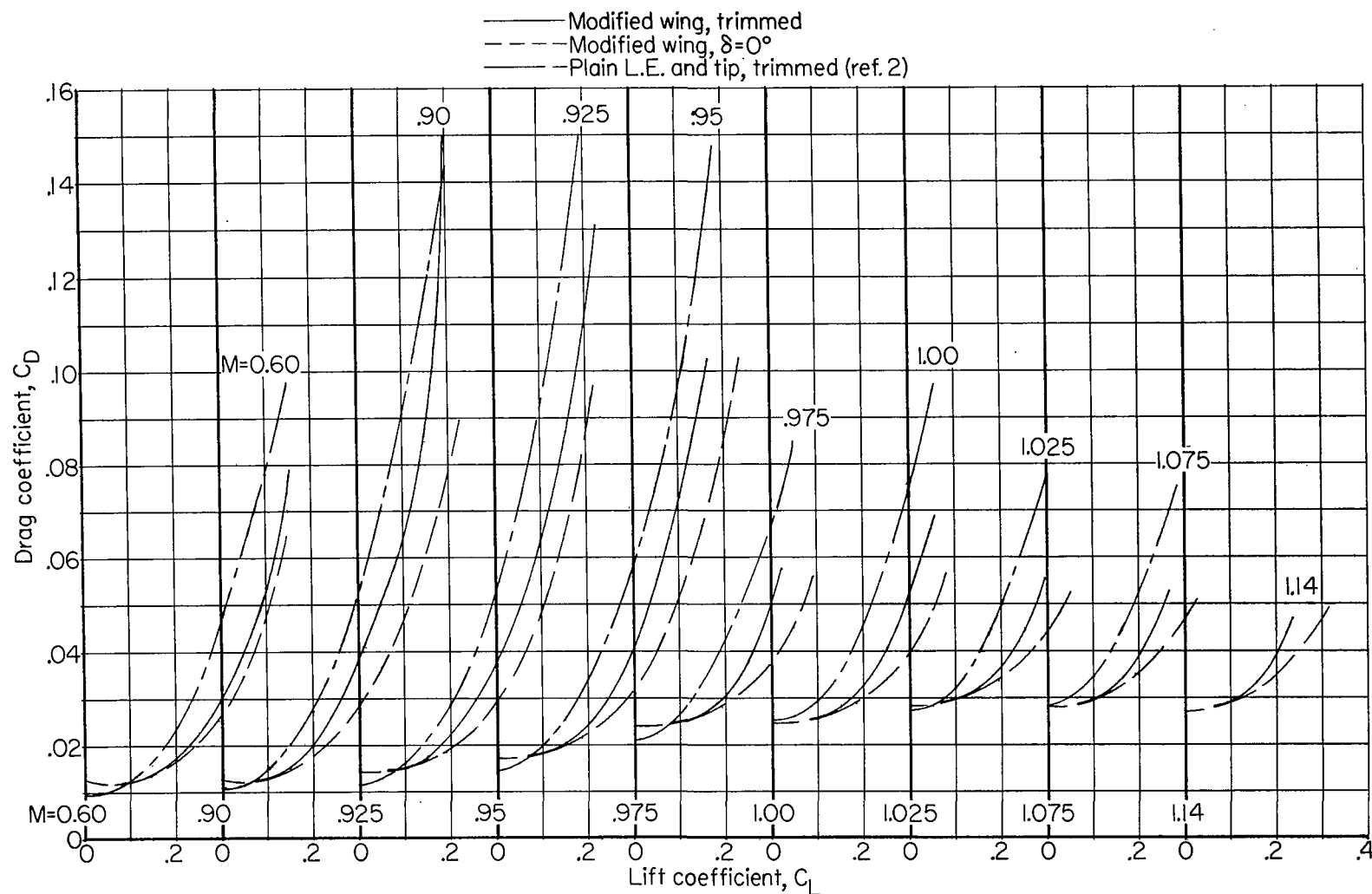


Figure 17.- Trimmed lift-drag polars compared for the Convair F-102 with and without wing modifications. Internal drag removed.

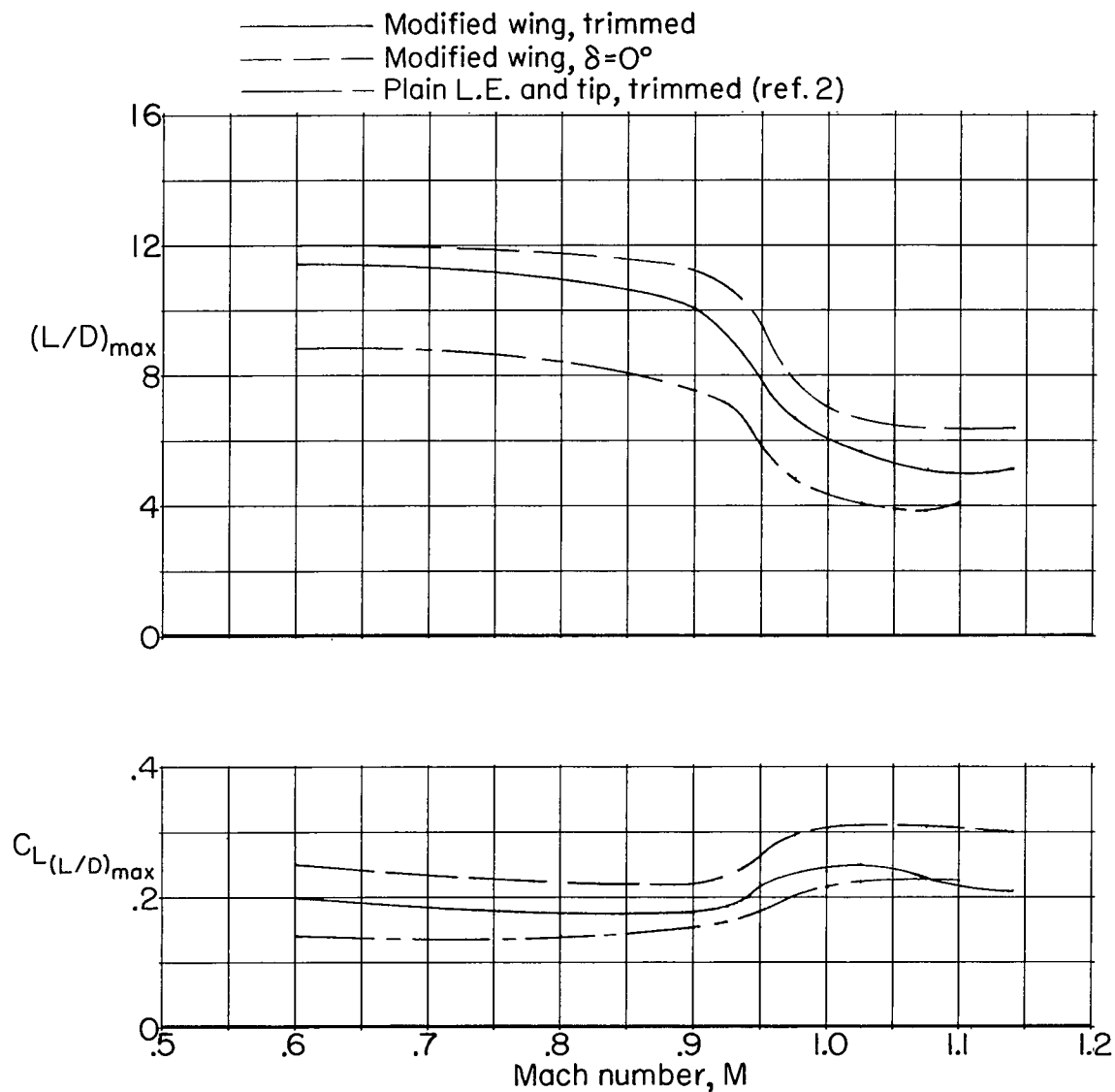


Figure 18.- Maximum trimmed lift-drag ratio characteristics compared for the Convair F-102 with and without wing modifications. Internal drag removed.

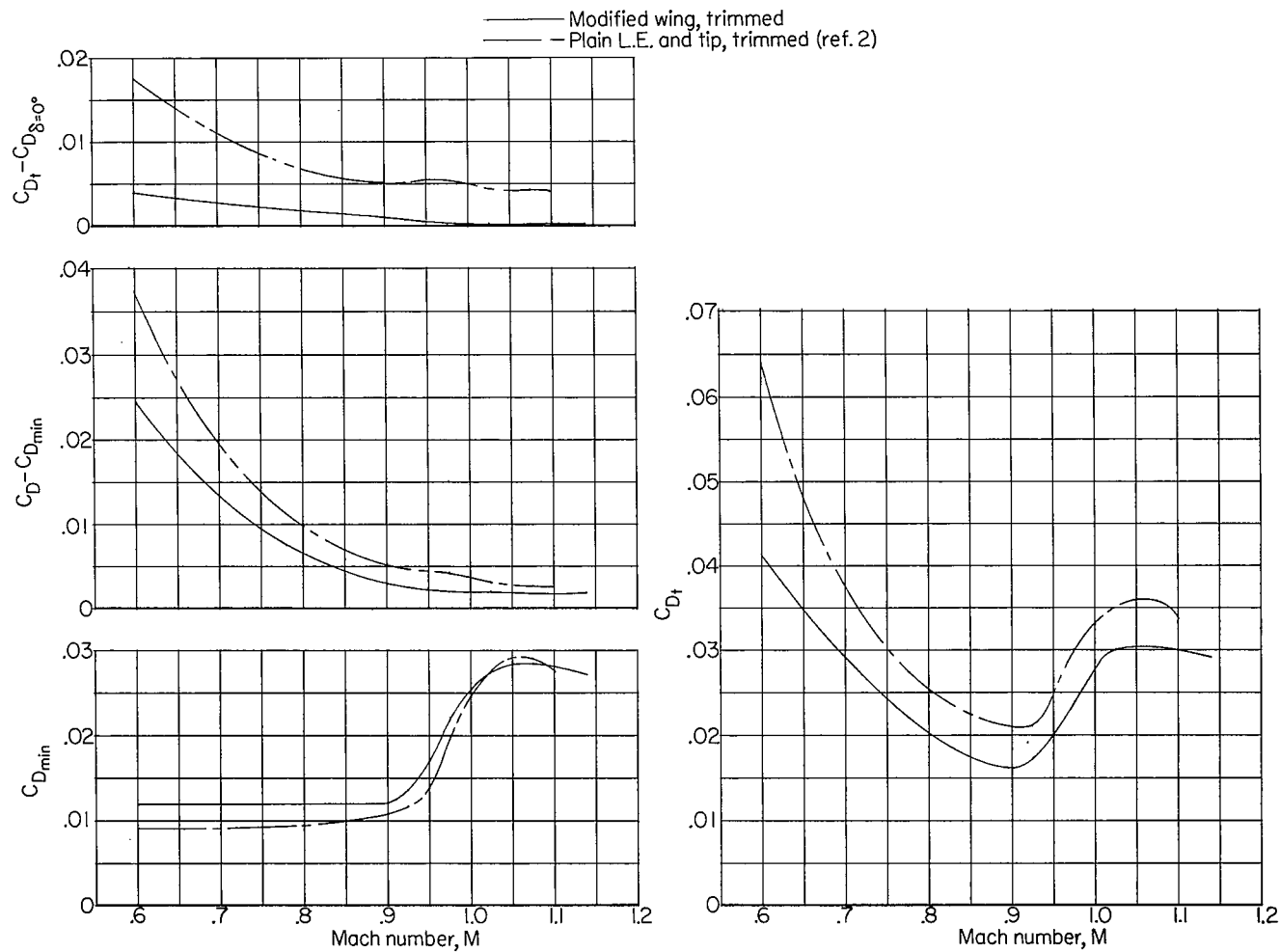


Figure 19.- Drag-coefficient breakdown compared for the Convair F-102 with and without wing modifications for trimmed level flight at 40,000 feet for a wing loading of 35.4 pounds per square foot. Internal drag removed.

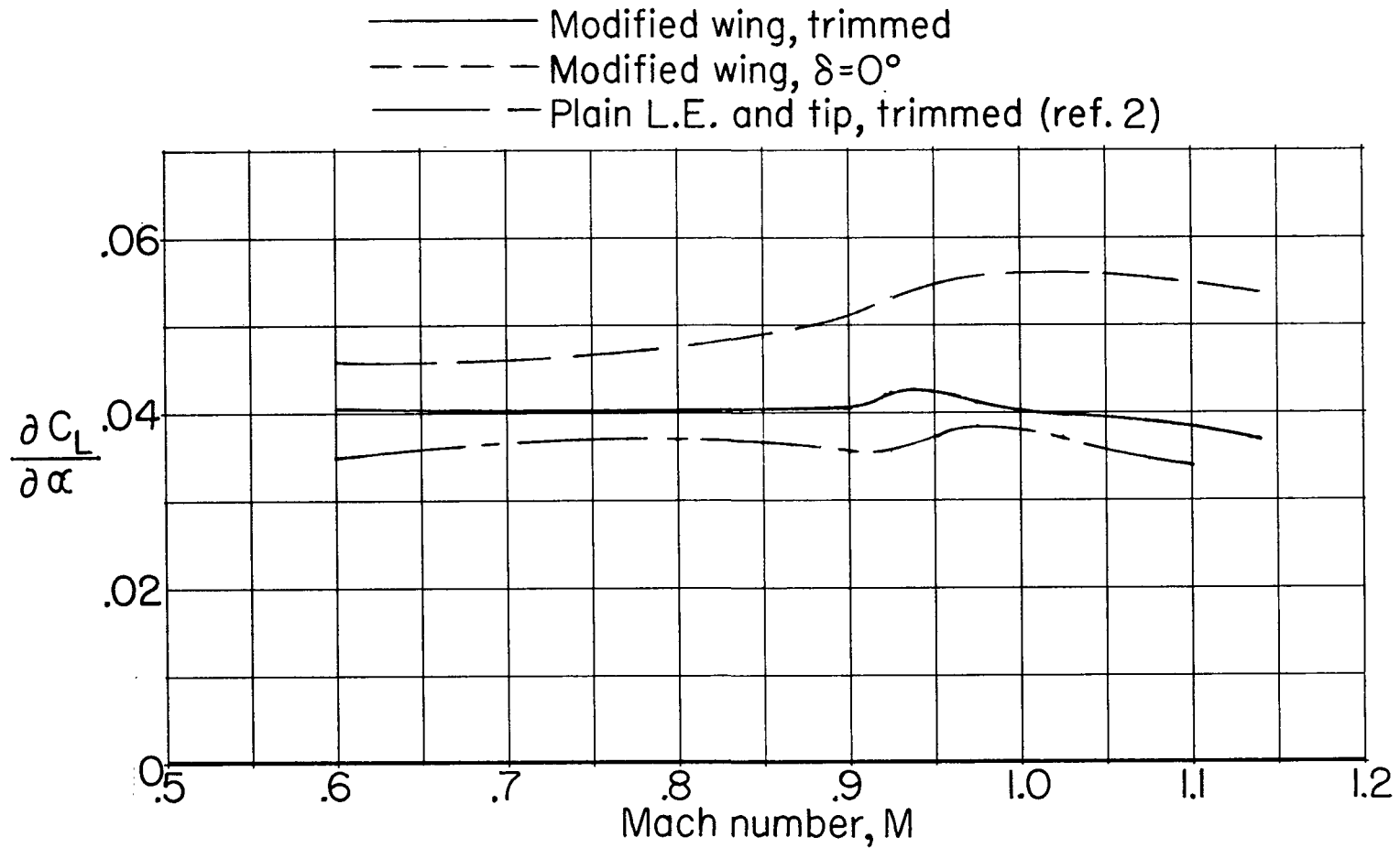


Figure 20.- Lift-curve slopes compared for the Convair F-102 with and without wing modifications.

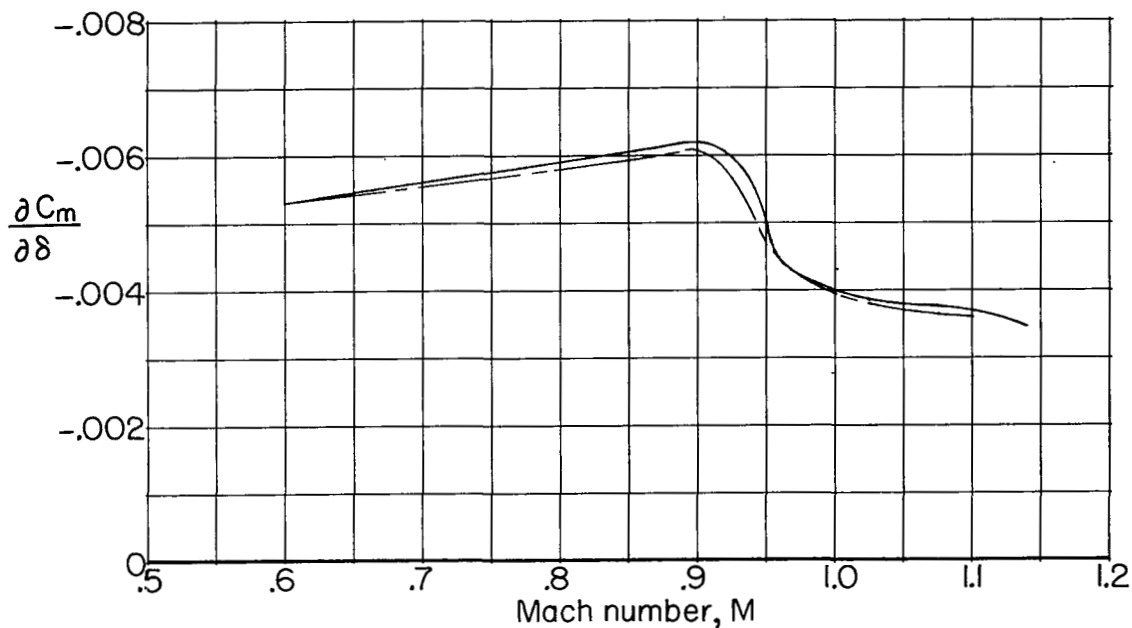
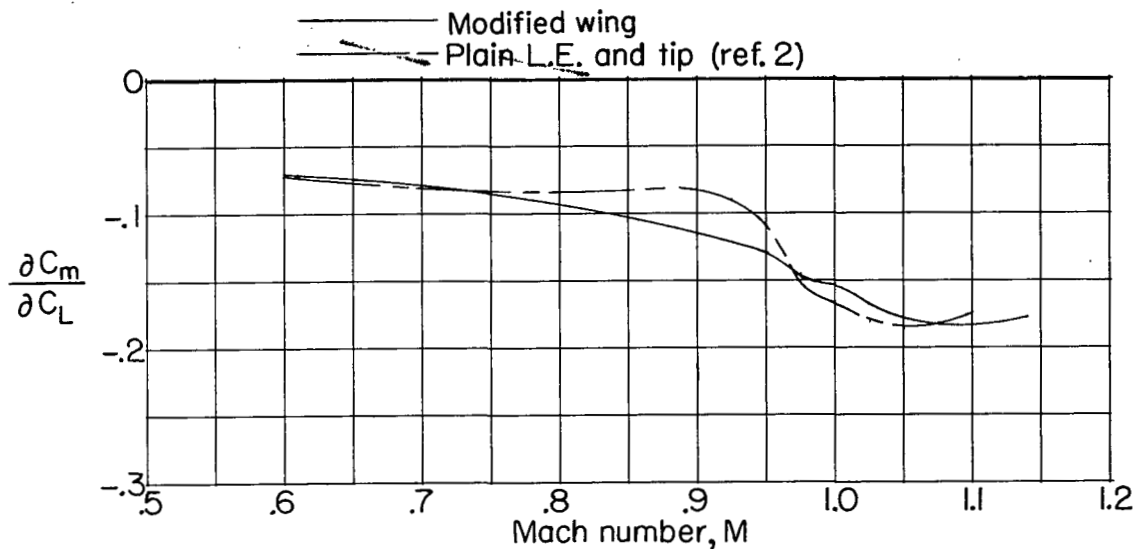


Figure 21.- The trimmed longitudinal-stability parameter at an altitude of 40,000 feet and the average elevator pitch effectiveness parameter compared for the Convair F-102 with and without wing modifications.

NASA Technical Library



3 1176 01438 6792

CONFIDENTIAL